



*UNIVERSITÀ POLITECNICA DELLE MARCHE*

Scuola di Dottorato di Ricerca della Facoltà di Medicina e Chirurgia

Corso di Dottorato in Salute dell'Uomo

***Senescent macrophages in adipose tissue:***

***ex vivo and in vitro characterization***

Dottoranda:

***Giulia Maticchione***

Docente tutor:

***Prof.ssa Fabiola Olivieri***

***XXXII Ciclo***

***Triennio Accademico 2016/2019***

# *Index*

<b>Summary</b> .....	<b>1</b>
<b>1. Introduction</b> .....	<b>5</b>
1.1 Obesity: distribution and classification .....	5
1.2 The adipose organ: anatomy, morphology and function .....	7
1.2.1 Macrophages in adipose tissue .....	10
1.2.2 Obesity-induced adipose tissue dysfunction.....	13
1.3 Type 2 Diabetes.....	17
1.4 Aging and cellular senescence.....	20
1.4.1 The hallmarks of cellular senescence: focus on telomere shortening.....	22
1.4.2 Senescent cell markers .....	24
1.4.3 Senescence-associated secretory phenotype (SASP) .....	25
<b>2. Aim of the work</b> .....	<b>29</b>
<b>3. Materials and methods</b> .....	<b>34</b>
3.1 Patients .....	34
3.2 SA- $\beta$ -Galactosidase staining for fresh organ.....	35
3.3 Paraffin embedding .....	36
3.4 Counting of $\beta$ -Gal <sup>+</sup> cells in tissue sections.....	36
3.5 IHC for CD68.....	36
3.6 THP-1 culture.....	37
3.7 Macrophage polarization and hyperglycemia treatment .....	38
3.8 HMADs differentiation .....	38
3.9 Trans-well co-culture assay.....	39
3.10 SA- $\beta$ -Galactosidase staining for cell culture.....	39
3.11 Cytokine production.....	39
3.12 RNA isolation from adipose tissue and cell culture .....	39
3.13 Quantitative RT-PCR of mature miRNAs.....	40
3.14 Quantitative RT-PCR of mRNA .....	40
3.15 DNA isolation.....	41
3.16 Telomere length measurement .....	41
3.17 Protein extraction and immunoblotting.....	42
3.18 Flow cytometer analysis.....	42
3.19 Fluorescence detection of SA- $\beta$ -Gal activity .....	43
3.20 Statistical analysis .....	43
<b>4. Results</b> .....	<b>44</b>

4.1	Histological analysis.....	44
4.1.1	Accumulation of SA- $\beta$ -Gal <sup>+</sup> cells in obese abdominal VAT.....	44
4.1.2	Senescent cells in adipose tissue are positive for CD68 pan-macrophage marker.....	46
4.2	In vitro analysis .....	47
4.2.1	Hyperglycemia triggers a mixed M1/M2 polarization in PMA-induced macrophages.....	47
4.2.2	HgSMs show features of senescent cells.....	49
4.2.3	Human multipotent adipose tissue-derived stem (hMADS) cells differentiate into white adipocytes.....	51
4.2.4	HgSMs move towards a pro-inflammatory phenotype when cocultured with adipocytes .	52
4.2.5	Adipocytes exhibit a high inflammation burden when coculture with HgSMs, only at mRNA expression level.....	54
4.3	Cytofluorimetric analysis .....	57
4.3.1	Age-related M1/M2 phenotype changes in circulating monocytes from healthy individuals and AMI patients.....	57
4.3.2	Evaluation of senescence in circulating monocyte subsets and their M1/M2 phenotype by flow cytometry .....	61
4.4	Circulating miR-146a shows age- and gender-specific trajectories in healthy aging and type 2 diabetes.....	63
4.5	Modulation of plasmatic $\beta$ -Galactosidase activity in healthy subjects is age-dependent.....	63
4.6	miR-222 and NF-light as new CSF biomarkers in age-related dementias .....	64
<b>5.</b>	<b>Discussion and Conclusion .....</b>	<b>65</b>
<b>6.</b>	<b>References .....</b>	<b>71</b>

## *Summary*

Age-related disorders (ARDs) have become widespread throughout the world and the leading cause of death in developed countries. In the past century, the rapid changes in lifestyle have created favorable conditions for survival but also access to nutrient-rich food and a sedentary lifestyle (Franceschi 2017). The most common ARDs are characterized by chronic, sterile, low-grade inflammation, named *inflammaging*. The grade of *inflammaging* in a subject depend on the genetic make-up and epigenetic conditions.

Obesity is a powerful risk factor for many age-related diseases, such as hypertension, dyslipidemia, cardiovascular complications, impaired glucose tolerance or Type 2 diabetes mellitus (T2DM). In this regard, insulin resistance is a major cause that leads to T2DM progression. Evidence showed that inflammation has a crucial role in the development of insulin resistance, particularly due to macrophages infiltration into visceral adipose tissue in obese states.

Recently, senescent cells have been found to accumulate in adipose tissue of obese and diabetic humans and mice (Minamino, Orimo et al. 2009, Villaret, Galitzky et al. 2010, Schafer, White et al. 2016) but it is unclear if their presence is a causal driver.

Cellular senescence is described as the phenomenon whereby cells irreversibly lose their replicative capacity and undergo morphological and functional modifications. The most relevant functional modification of a senescent cell is that it remains metabolically active and acquires a pro-inflammatory secretory phenotype named secretory phenotype associated with senescence (SASP)(Coppe, Patil et al. 2008).

Therefore, the SASP leads to the accumulation and propagation of inflammatory molecules such as cytokines, microRNAs and DNA fragments both at paracrine and systemic level helping to perpetuate and amplify the inflammatory process.

Damage-related, inflammatory, oncogenic, and metabolic stimuli, can potentially induce a senescence response (Munoz-Espin and Serrano 2014).

However, the molecular bases on how obesity accelerates the aging of adipose tissue are only now beginning to come to light.

Analysis of obese mice adipose tissue revealed an increased level of ROS and DNA damage compared to lean mice. Moreover, adipose tissue showed features of senescence, such as a higher expression of senescence-associated  $\beta$ -galactosidase, p53 and p21 proteins.

Thus, overnutrition-resulted obesity accelerated DNA damage and aging (particularly telomere shortening) by stimulating ROS production. These alterations prompt inflammation and cytokine production in adipose tissue, which leads to insulin resistance locally and systemically (Ahima 2009).

Despite the number of senescent cells is relatively small in human tissues, they have been associated with multiple diseases of aging, emerging as useful therapeutic targets for ARDs (Roos, Zhang et al. 2016, Farr, Xu et al. 2017, Schafer, White et al. 2017, Musi, Valentine et al. 2018).

In this framework, novel drugs termed senolytics have been identified to diminish senescent cell numbers in tissues (Kirkland, Tchkonina et al. 2017).

Senolytics mechanism is based on blocking survival pathways, such as PI3K/AKT, p53/p21/serpin, HIF1 $\alpha$ , and BCL-2/BCL-XL family components, which allow senescent cells to escape from apoptosis (Zhu, Tchkonina et al. 2015, Zhu, Tchkonina et al. 2016).

Of note, a recent paper has demonstrated that the elimination of senescent cells by treatment with two senolytics (dasatinib and quercetin) in obese mice alleviates metabolic and adipose tissue dysfunction. In particular, they found glucose tolerance improvement, insulin sensitivity enhancing, low level of circulating inflammatory mediators, and adipogenesis promotion.

Thus, targeting senescent cells could be a novel therapeutic target for obesity-induced metabolic dysfunction (Palmer, Gustafson et al. 2019).

However, it is still unclear which cells *in vivo* carry these markers of senescence (Hall, Balan et al. 2016).

Certainly the pathogenesis of a plethora of ARDs have been associated with the accumulation of macrophages as happens in cancer (Noy and Pollard 2014), atherosclerosis (Moore and Tabas 2011), diet-induced obesity and insulin resistance (Bu, Gao et al. 2013), fibrosis (Braga, Agudelo et al. 2015) and osteoarthritis (Sun, Friis et al. 2016). More recently, it has been demonstrated that senescent cells have been involved in the same diseases (Baker, Childs et al. 2016, Schafer, White et al. 2017).

Macrophages are an important component of innate immunity (Wynn and Vannella 2016), and cooperate with adaptive immune cells. Macrophages can acquire different phenotypes depending on their function and gene expression patterns. Mainly two opposite phenotypes are more thoroughly characterized: classical (M1) and alternative (M2) activated macrophages (Mantovani, Sica et al. 2004). M1 phenotype can be induced by LPS and type-1 cytokines (e.g. IFN- $\gamma$ ) and is associated with pro-inflammatory responses to bacteria and viruses. On the contrary, polarization towards M2 can be induced by type 2 cytokines (e.g. IL-4 and IL-13) and is related to anti-inflammatory response and regulation of wound healing (Roszer 2015). Notably, macrophages are characterized by high phenotypic plasticity and exhibit a variety of mixed M1/M2 phenotypes allowing for rapid response and adaptation to several microenvironmental signals (Martinez and Gordon 2014, Murray 2017).

Macrophages can exhibit some features of SCs, such as p16(Ink4a) positivity, and  $\beta$ -galactosidase<sup>bH6</sup> activity (the commonly accepted biomarkers of senescent cells).

Indeed, systemic clodronate treatment of old mice that showed an elevated number of senescent cells in their tissues led to the reduction of these cells, indicating that a significant proportion of senescent cells in an aged organism is actually a subclass of macrophages. Thus, macrophages

expressing senescence markers were found to occur naturally within the adipose tissue of chronologically aged mice.

However, the relative impact of senescent macrophages and senescent cells in age-related diseases is currently unclear, due to the lack of a consistent characterization of the macrophage phenotype in an aged milieu (Hall, Balan et al. 2017). Understanding the regulatory mechanisms of adipose tissue macrophages polarization and what trigger senescence can be relevant to develop new approaches to prevent the development of obesity-related metabolic disorders and to identify therapeutic targets for anti-aging treatment (**fig.1**).

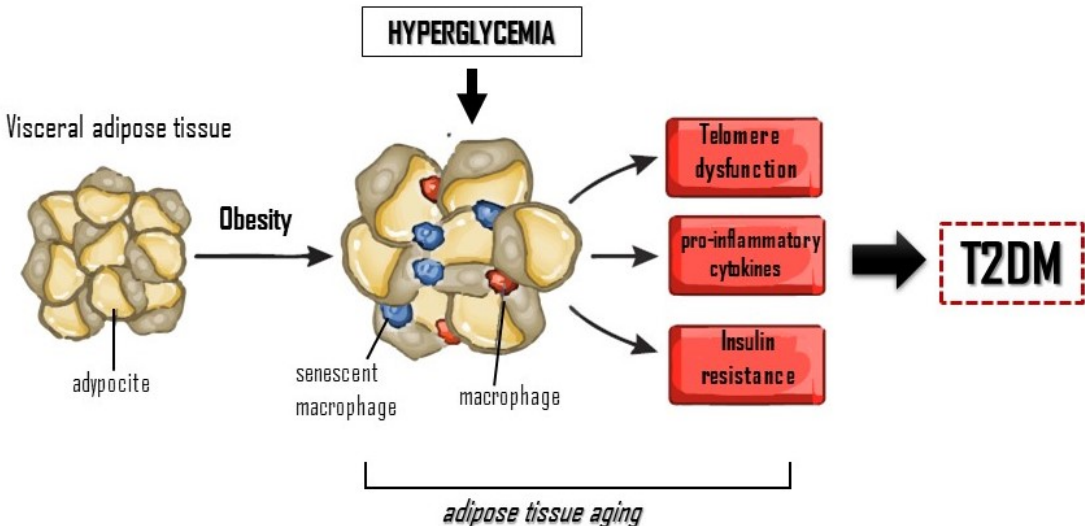


**Figure 1. Proposed mechanism of senescent macrophage- driving T2DM in obesity.** Macrophages accumulate into adipose tissue during obesity and can eventually become senescent, triggered by hyperglycemia. Senescence leads to telomere shortening, pro-inflammatory cytokines propagation and then insulin resistance, thus establishing T2DM (modified from Ahima 2009).

# 1. Introduction

## 1.1 Obesity: distribution and classification

Obesity is dramatically becoming a worldwide health concern and a large economic burden in all countries, as lead to increased risk for most diseases, particularly diabetes, cardiovascular diseases and cancers (Rtveladze, Marsh et al. 2014). Keaver et al. proposed that overweight and obesity could reach 89% levels in males and 85% levels in females within Ireland population by 2030, whereas the Organization for Economic Co-operation and Development (OECD) state that until 2030 the obesity rates are expected to grow and notably United State, Mexico and England will reach respectively a level of 47%, 39% and 35% of obese subject in the population (**fig. 2**).

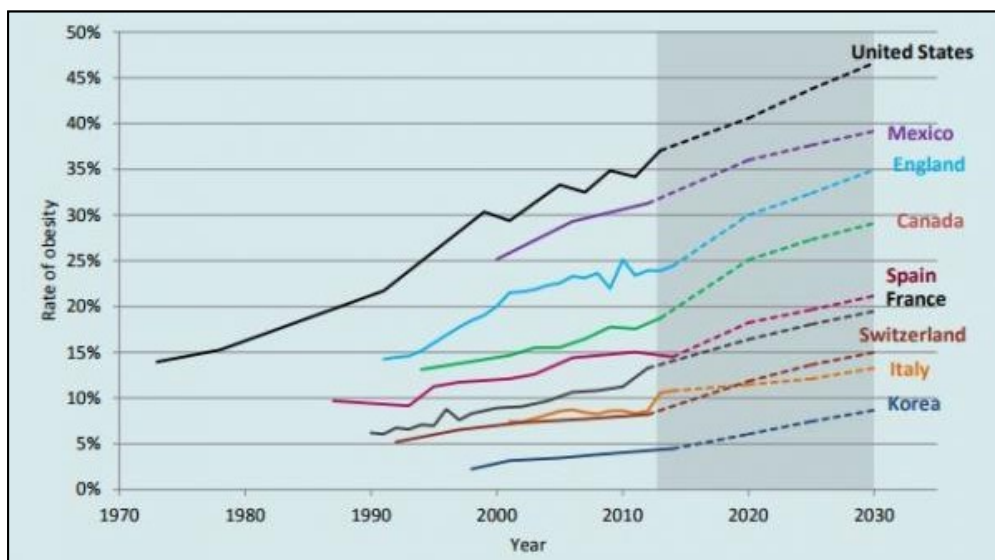


**Figure 2. Worldwide rate of obesity by 2030.** Obesity rates are expected to grow, and United State, Mexico and England will reach respectively a level of 47%, 39% and 35% of obese subjects in the population (OECD obesity update 2017).

Classification of obesity is based on BMI (Body Mass Index), which is body weight in kilograms divided by the height in meters squared ( $\text{kg}/\text{m}^2$ ). To date, this method is standardized and internationally accepted. Conforming to BMI, it is possible to discriminate among five different



categories namely normal range (18.5-24.9 kg/m<sup>2</sup>), overweight (25.-29.9 kg/m<sup>2</sup>), class 1-obesity (30.0-34.9 kg/m<sup>2</sup>), class 2-obesity (35.0-39.9 kg/m<sup>2</sup>) and class 3-obesity (equal or greater 40 kg/m<sup>2</sup>). Grade 3 obesity or grade 2 obesity with significant obesity-related co-morbidities are defined as a condition of morbid obesity (Ashwell, L. Mayhew et al. 2014).

Life expectancy widely decreases in obese in a range between 3.3 and 18.7 years (Leung et al. 2015). Amongst individuals with BMI above 25, each 5 kg/m<sup>2</sup> higher of BMI, there is a 30% or higher overall mortality, which is mainly due to increased risk of cardiovascular death as 40% (Engin 2017).

Nevertheless, the class distribution by BMI calculation does not account for body composition. Thus, another measurement to predict obesity risk is the body adiposity index (BAI) that takes into consideration height and hip circumference dimensions.

The content of body fat, as well as the distribution of adipose tissue, are considered a critic indicators of health risk, as total fat mass is not the principal feature that explains the increased metabolic risk in obese. Rather, metabolic health is dependent on the anatomical site where the excessive calories are stored together with adipose tissue function.

Indeed, visceral adiposity accumulation is associated with insulin resistance (IR), whereas the distribution of body fat in different anatomical districts, such as subcutaneous fat, is metabolically less important (Kahn, R.L. Prigeon et al. 2001). For example, the surgical removal of subcutaneous adipose tissue in the abdomen (abdominal liposuction), is not effective in ameliorating obesity-associated metabolic abnormalities.

Moreover, abdominal adipose tissue accumulation in the upper body region is associated with the development of obesity-related comorbidities and even all-cause mortality. On the contrary, fat accumulated in the gluteofemoral body region is linked to a protective lipid and glucose profile leading to a decreasing in cardiovascular and metabolic disease prevalence (Snijder, Zimmet et al.

2004). These differences in disease risk are due to strikingly divergent functional properties of these adipose tissue depots (Goossens 2017).

## ***1.2 The adipose organ: anatomy, morphology and function***

Adipose tissue creates a large organ with specific anatomy and complex cytology, supplied by nerve and vasculature and high physiological plasticity (Cinti, Zingaretti et al. 2001, Cinti 2011). Through the body several depots are mainly located in two compartments: subcutaneous depots are beneath the skin and visceral depots are in the trunk, surrounding internal organs (e.g. stomach, liver, intestine, kidney.) Thus, adipose tissue is considered a multi-depot organ (Cinti 2005) that is involved in immune responses, thermogenesis, lactation and providing energy for metabolism. Adipocytes are the main parenchymal cells of the adipose tissues, and they can be grouped in two types, easily distinguishable by morphology: white and brown cells.

White adipocytes have a spherical shape and a cytoplasmic lipid droplet enlarging for 90% of their volume and comprising a single and a 'squeezed' nucleus, whereas brown adipocytes are polygonal and constituted of several cytoplasmic lipid droplets, a roundish nucleus and numerous large mitochondria.

Furthermore, adipocytes are quite different even in their physiology: white adipocytes store energy for the organism metabolism, whereas brown adipocytes burn energy for thermogenesis (Cinti 2012) (**Fig.3**).

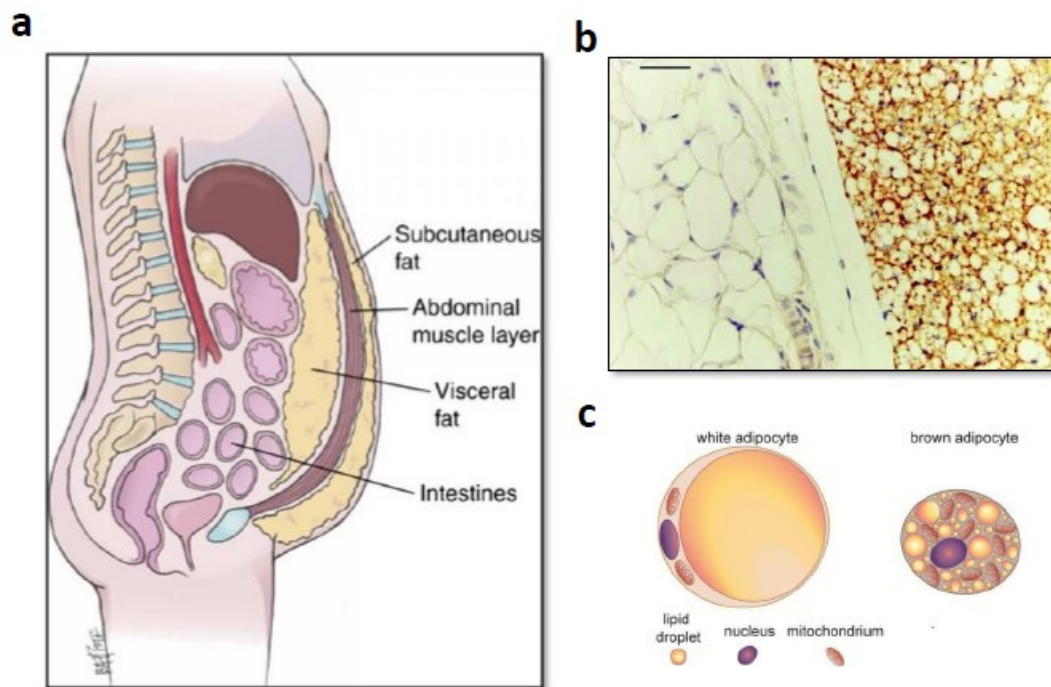


**Figure 3. The adipose organ.** a) Anatomy of the adipose tissue depots: the two main compartments are subcutaneous and visceral fat. b) histology of the adipose tissue: white and brown fat can be easily distinguished by morphology. c) white and brown adipocyte: on the left a white adipocyte with the unique lipid droplet, on the right the brown adipocyte with several small lipid droplet.

Apart from adipocytes, which comprise the highest cell percentage, adipose tissue contains the stromal vascular fraction (SVF) of cells including preadipocytes, fibroblasts, immune cells (mainly adipose tissue macrophages) and vascular endothelial cells, as contained many small blood vessels. In addition to energy storage and thermoregulation, fat provides several and important functions such as mechanical protection, tissue regeneration, and immune and endocrine activity. The main role is the storage of calorically dense fatty acids, that are cytotoxic and highly reactive. Adipocytes sequestered these molecules transforming them in the less reactive triglycerides within fat droplets, by protecting from systemic lipotoxicity (Tchkonia, Giorgadze et al. 2006).

Another characteristic of adipose tissue is the capability to accommodate the wide fluctuation in nutrient availability, by rapid and extensive changes in size, especially within subcutaneous fat, which is not subject to the anatomic constraints. The fat organ can grow through changes in fat cell size or number that vary in magnitude.

Interestingly, adipose tissue location (beneath the skin and around vital organs) is strategic, as can protect against infection and trauma. Indeed, bacterial and fungal infections of fat, as well as metastases, are quite unusual and likely related to the immune cell activity and high fatty acid concentrations in fat tissue that are lethal to pathogens and non-adipose cell types (Tchkonina, Morbeck et al. 2010). Adipose tissue is an active endocrine organ secreting local and systemic hormones (such as leptin and adiponectin), cytokines (such as TNF- $\alpha$  and interleukin-6) interacting with the immune system and various growth factors: insulin-like growth factor (IGF-1) and transforming growth factor (TGF- $\beta$ ) (Wellen and Hotamisligil 2003).

Adipokines (hormones, cytokines and other proteins with signaling properties) are synthesized by adipocytes and regulate appetite, angiogenesis, metabolism of glucose and fatty acids, as well as inflammatory and immune reactions (Trayhurn and Wood 2004).

Adiponectin is the most abundant hormone in circulation (0.05% of serum proteins) secreted after activation of the nuclear receptor Peroxisome Proliferator-Activated Receptor- $\gamma$  (PPAR- $\gamma$ ) in adipocytes mainly to enhance metabolism of glucose and fatty acids (reduction of FFA concentration) in liver and muscle and increasing insulin sensitivity (Cowey and Hardy 2006, Piatkiewicz and Czech 2011). Adiponectin has anti-inflammatory activity and negatively regulates angiogenesis (Brakenhielm, Cao et al. 2004). Moreover, hypoxia induces a low level of adiponectin within the tissue.

Leptin is known as the hormone that gives a feeling of satiety by reducing food intake (Gorska, Popko et al. 2009) as it increases insulin sensitivity and lipolysis. Fat is the major source of leptin,

thus obese become hyperleptinemic for the development of leptin resistance and more susceptible to metabolic disorders (Cowey and Hardy 2006).

In addition, adipocytes secrete proangiogenic factors, mainly the vascular endothelial growth factor (VEGF). VEGF is stimulated by hypoxia and involved in angiogenesis. Recently, a study on obese individuals demonstrated an increase in serum VEGF positively correlated with visceral adiposity accumulation (Miyazawa-Hoshimoto, Takahashi et al. 2003).

Besides, adipose tissue expresses numerous miRNAs which major function is to stimulate or inhibit the differentiation of adipocytes, and to regulate specific metabolic and endocrine functions. However, it has been shown that the expression of only few miRNAs are altered in individuals with obesity and type 2 diabetes mellitus or are differentially expressed in various adipose depots (Arner and Kulyte 2015).

### ***1.2.1 Macrophages in adipose tissue***

Macrophages are an essential component of innate immunity, playing a central role in inflammation and host defense along with tissue remodeling in ontogenesis and metabolic functions regulation (Sica, Rubino et al. 2007, Biswas and Mantovani 2010, Gordon, Rao et al. 2010). A consistent diversity and plasticity characterized monocyte-macrophage lineage. Distinct functional phenotypes can be acquired in response to different environmental stimuli: precisely, macrophages may undergo classical M1 activation (stimulated by TLR ligands and IFN- $\gamma$ ) or alternative M2 activation (stimulated by IL-4/IL-13).

The M1 phenotype is distinguished by a high level of proinflammatory cytokines expression, high reactive nitrogen, and oxygen intermediates production, Th1 response promotion, and strong microbicidal activity. In contrast, the M2 phenotype is involved in parasite containment and immunoregulatory functions as well as the promotion of tissue remodeling due to an efficient phagocytic activity (Mantovani, Sizzani et al. 2002, Sica and Mantovani 2012). Both M1 and M2

macrophages widely consume arginine: M2 macrophages metabolize arginine to ornithine and urea (Morris 2010). Ornithine is essential in many repair processes, such as cell proliferation and collagen biosynthesis. M1 macrophages metabolism of arginine produces toxic NO. These macrophages induce the enzyme NO synthase (iNOS), that produces large amounts of NO and citrulline. NO is not only cytotoxic, but it generates many downstream toxic metabolites that together constitute the M1 killing machinery (Ley 2017). (fig. 4)

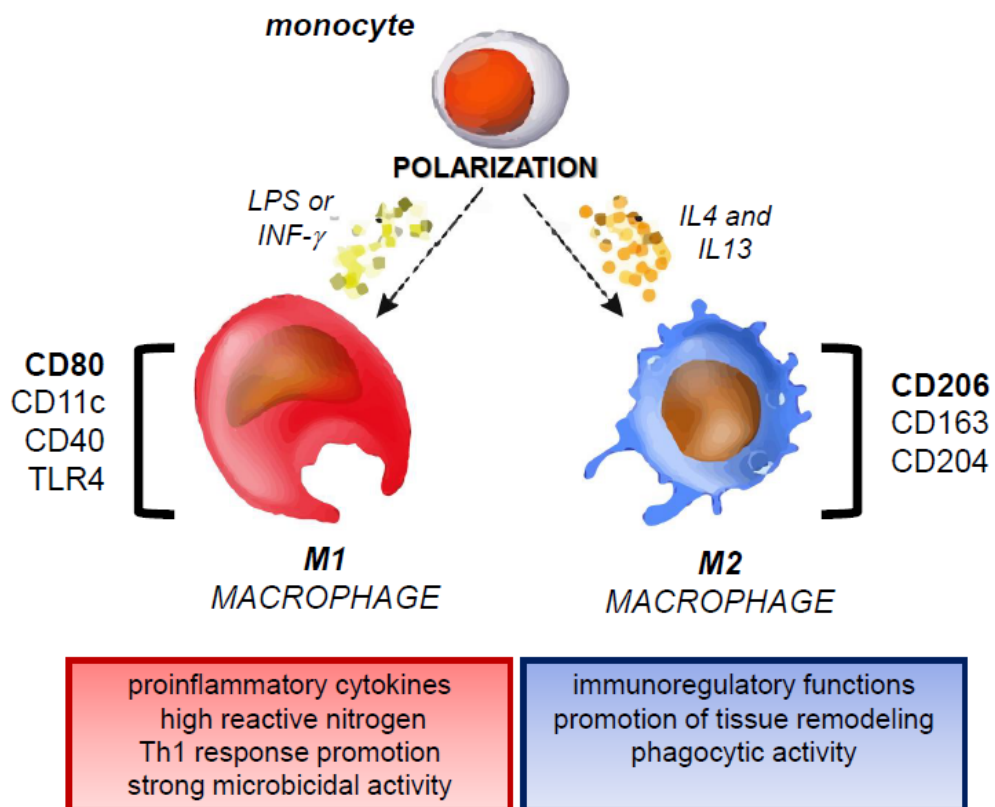


**Figure 4. Macrophage differentiation from monocyte.** On the left, macrophages undergo classical M1 activation (stimulated by TLR ligands or IFN- $\gamma$ ). On the right, alternative M2 activation (stimulated by IL-4/IL-13).

Adipose tissue macrophages (ATMs) have been recognized as important elements in immune function and inflammation (Weisberg, McCann et al. 2003). However, in human the different ATM phenotypes and the polarization mechanisms remain still to deepen.

Studies on mice bone marrow transplantation have established that most macrophages found in the adipose tissue are derived from blood monocytes (Weisberg, McCann et al. 2003); a concept confirmed by in vivo monocyte labeling (Lumeng, Bodzin et al. 2007). Three subsets of circulating monocytes have been identified in humans, based on the relative surface expression of LPS co-receptor CD14 and FC $\gamma$ III receptor CD16.

Classical monocytes (CD14<sup>++</sup>CD16<sup>-</sup>) represent approximately 80% of the total population, whereas monocytes expressing CD16, which account for about 20%, have been further classified into two subtypes: non-classical (CD14<sup>++</sup>CD16<sup>+</sup>) and intermediate (CD14<sup>low</sup>CD16<sup>+</sup>) monocytes (Ziegler-Heitbrock, Ancuta et al. 2010). Macrophage differentiation from monocytes occurs in tissues in concomitance with the acquisition of a functional phenotype depending on the local environment.

Two different phenotypes of ATMs have been already well-characterized: classically activated pro-inflammatory ATMs (M1) and alternatively activated anti-inflammatory ATMs (M2). Indeed, resident M2 ATMs are predominantly observed in lean animal models to contribute to the maintenance of the homeostasis of adipose tissue. On the contrary, obesity induces the secretion of monocyte chemoattractant protein 1 (MCP-1), a chemotactic molecule, from hypertrophic adipocytes, resulting in circulating monocytes recruitment into adipose tissue and their differentiation into an M1 phenotype (Dalmas, Clement et al. 2011). Indeed, the accumulation of proinflammatory ATMs in mice fed a high-fat diet was markedly observed (Lumeng, Deyoung et al. 2007) and this phenotypic M2 to M1 switch is crucial in adipose tissue to determine insulin resistance in obese mice.

However, in human ATMs polarization in obese individuals underlined a more complex modulation compared to mouse models. It has been reported M2 polarization in ATMs producing proinflammatory mediators (Bourlier, Zakaroff-Girard et al. 2008), whereas another study suggested a mixed M1/M2 phenotype increased in obese subjects that correlated with insulin resistance. Notably, Kratz and colleagues (Kratz, Baars et al. 2013) demonstrated that glucose, insulin, and palmitate trigger metabolic activation pathways and contribute to ATM polarization. Little is known about the regulation of ATM polarization and further investigations are needed.

To date, several cell surface markers of human M1 and M2 ATMs have been reported.

CD11c, CD40, CD80, HLA-DR, and TLR4 are considered to be suitable markers of human M1 ATMs, whereas, CD163, CD204 (macrophage scavenger receptors), and CD206 (mannose receptor) are known cell surface markers of M2 ATMs.

Interestingly Komahara et al. reported that only CD163 was upregulated by IL-10 treatment, which induces M2 polarization in human monocyte-derived macrophages and therefore can be a useful marker to represent M2 ATMs (Komohara, Fujiwara et al. 2016).

### **1.2.2 Obesity-induced adipose tissue dysfunction**

Obesity is defined as an overabundance of white adipose tissue and it is associated with a low-grade inflammatory state that is characterized by increased circulating concentrations of inflammatory cytokines and acute-phase proteins. In particular, abnormally high deposition of visceral adipose tissue is known as visceral obesity. Indeed, this body composition phenotype is associated with several diseases such as metabolic syndrome, cardiovascular disease and cancer (Shuster, Patlas et al. 2012).

As already explained above, adipose tissue itself is an inflammation site. It has been shown that in lean mice macrophages amount is estimated at less than 10% of the total cells of adipose tissue,



whereas in obese mice macrophages are more than 50% in adipose tissue (Dalmas, Clement et al. 2011).

Adipose tissue has a unique and extraordinary capacity to change its dimensions in response to nutritional intake taking advantage of remodeling mechanisms. Alterations include size, function, inflammatory state and whole-body distribution at the tissue level, whereas adipocytes change their extracellular matrix (ECM) composition, size and number, oxidative stress and adipokine secretion level. Vascularization and the inflammatory state of infiltrating immune cells were also modulated (Sun, Lopez-Verges et al. 2011). Two processes allow adipose tissue to expand: hypertrophy, that is the enlargement of pre-existing adipocytes by lipid accumulation, and hyperplasia in which the number of adipocytes increases through recruitment of pre-adipocytes from resident pools of progenitor cells.

Thus, hyperplasia involves the adipogenesis process, as *de novo* adipocyte was integrated (Rutkowski, Svoronos et al. 2015).

Obesity leads to a critically dysfunctional adipose tissue that is not capable of appropriately expand to store surplus energy, thereby resulting in ectopic fat deposition in other tissues through the whole body (such as the liver, skeletal muscle, and the endocrine pancreas). Consequently, progressive insulin resistance and risk of T2DM increase.

Adipocyte hypertrophy in obesity is accompanied by a shift to an adverse adipokine secretory profile typically together with a plethora of pro-inflammatory molecules, such as TNF- $\alpha$ , interleukin-1 $\beta$  (IL-1 $\beta$ ), interleukin-6 (IL-6), interleukin-8 (IL-8), leptin, resistin, as well as a reduction in anti-inflammatory factors, such as IL-10 and adiponectin (Lackey, Lazaro et al. 2016). Moreover, during obesity progression, chemotactic signals such as MCP1 recruit circulating monocytes, which infiltrate obese adipose tissue fueling inflammation. Resident ATM and newly recruited monocytes become polarized to pro-inflammatory M1 macrophages (Lumeng, Bodzin et

al. 2007). M1 ATM deregulate adipocyte signaling and insulin sensitivity mostly by secreting pro-inflammatory cytokines and forming ‘crown-like’ structures (CLSs) (Lackey, Lazaro et al. 2016). Indeed, hypertrophic adipocytes could eventually die and release the cellular contents into the extracellular space. This lead to induce an inflammatory response in macrophages that surround adipocytes displaying features of dead cells to form crown-like structures (CLSs) (Cinti 2005).

Dysfunctional obese adipose tissue shows a higher degree of fibrosis and hypoxia. Fibrosis is a pathological process characterized by an abundance of ECM proteins, particularly collagens (Ricard-Blum 2011). Indeed, the ECM is crossed with adipocytes to form a scaffold, and in obesity progression its rigidity, composition and remodeling is fundamental of the adipose tissue expansion.

Flexible ECM allows adipose tissue to freely expand in a healthy stress-free manner. This beneficial partitioning of excess fat is associated with improvements glucose and lipid homeostasis in whole-body (Khan et al, 2009).

On the contrary, if the ECM is inflexible, adipocytes result embedded and are not capable to appropriately store lipids in excess, which prevent adipose tissue growth and promotes lipotoxicity. It has been identified highly enriched collagen VI in ECM of adipose tissue (Iyengar, Hudis et al. 2015), which has a crucial role in the fibrotic component of obesity.

Hypoxia is a process occurring early in adipose tissue dysfunction and a major cause of ECM stress beginning. When adipose tissue starts to rapidly expand, it goes faster than its own neo-vascularization system, thus promoting a state of hypoxia (**fig.5**).

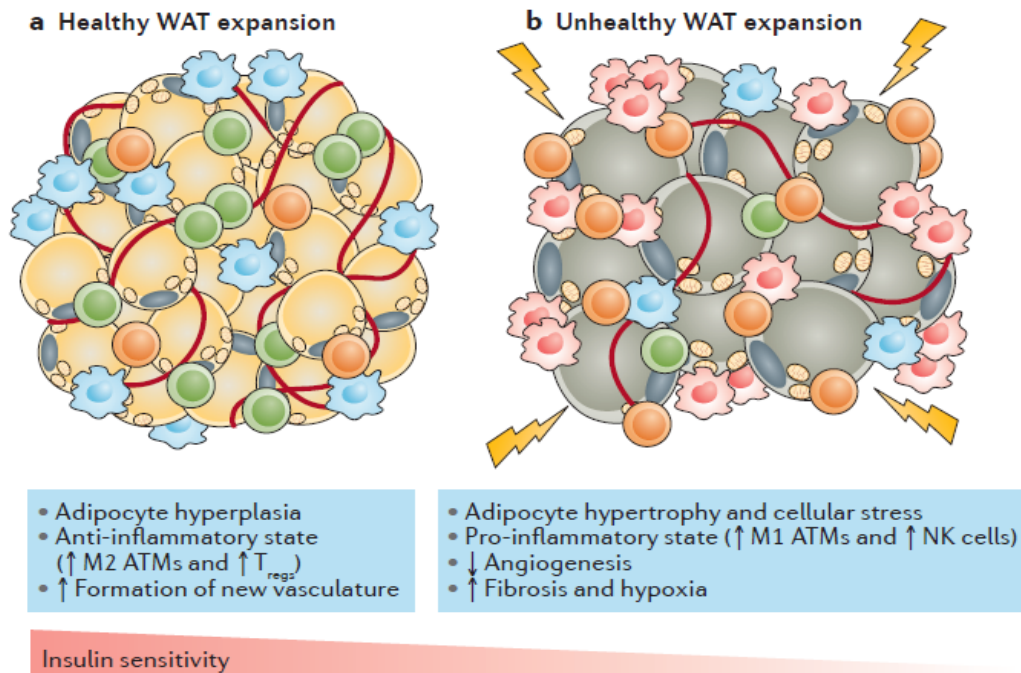


**Figure 5. Metabolically healthy white adipose tissue expansion versus unhealthy pathological expansion during the progression of obesity.** a) During healthy adipose tissue expansion, the tissue is in an anti-inflammatory state, in which there is sufficient vasculature to support the expansion and the adipocytes undergo hyperplasia. b) Unhealthy adipose tissue harbours enlarged hypertrophic adipocytes (grey cells) and also displays a heightened state of inflammation. The formation of new vasculature to support fat growth (red lines) is also impaired, and enhanced fibrosis and hypoxia are evident. Such events contribute to the development of insulin resistance (Kusminski, Bickel et al. 2016).

Notably, the transcription factor hypoxia-inducible factor 1 $\alpha$  (HIF1 $\alpha$ ) that is the ‘master regulator of oxygen homeostasis’ displays enhanced activity in obese fat (Krishnan, Danzer et al. 2012).

For example, HIF1 $\alpha$  overexpression in mice adipose tissue initiates fibrosis and local inflammatory events whereas its ablation correlates to metabolic improvements in diet-induced obesity (Kusminski, Bickel et al. 2016).

### 1.3 Type 2 Diabetes

The International Diabetes Federation affirmed that 382 million people were affected by diabetes in 2013 and disease prevalence is expected to rise to 592 million by 2035. Diabetes can be considered a worldwide epidemic, although 80% of diabetic people live in low-income and middle-income countries (Donath 2014).

Diagnosis of diabetes mellitus is based on glycated hemoglobin (A1C) criteria or plasma glucose levels, either the fasting plasma glucose (FPG) or the 2-h plasma glucose (2-h PG) value, the latter after a 75-g oral glucose tolerance test (OGTT). Particularly fasting is defined as no caloric intake for at least 8 h whereas glycated hemoglobin measured the level of glucose chemically linked to hemoglobin, namely the average blood sugar concentration for the past two to three months.

Criteria by World health organization (WHO) defined diabetes mellitus condition when A1C  $\geq 6.5\%$  or FPG  $\geq 126$  mg/dL (7.0 mmol/L) or 2-h PG  $\geq 200$  mg/dL (11.1 mmol/L) during an OGTT (American Diabetes Association, 2015) (**fig.6**).

	HbA1c (percent)	Fasting Plasma Glucose (mg/dL)	Oral Glucose Tolerance Test (mg/dL)
Diabetes	$\geq 6.5$	$\geq 126$	$\geq 200$
Normal	$\sim 5.7$	$\leq 99$	$\leq 139$

**Figure 6. Diagnosis criteria of diabetes mellitus by World health organization (WHO).** Diabetes mellitus condition is considered when A1C  $\geq 6.5\%$  or FPG  $\geq 126$  mg/dL (7.0 mmol/L) or 2-h PG  $\geq 200$  mg/dL (11.1 mmol/L) during an OGTT (modified from American Diabetes Association (2012)).

Cellular and molecular mechanisms responsible for type 2 diabetes are mainly related to glycemia regulation (Stumvoll, Goldstein et al. 2005). Glucose homeostasis is maintained by a balance between the production of glucose in the liver (dependent on glycogenolysis and gluconeogenesis pathways) during fasting and glucose metabolism and glycogen synthesis mainly in skeletal muscle during feeding.

The key hormone for this process is insulin, secreted by the beta cells of the pancreas. When nutrient uptake occurs, the secretion of insulin inhibits hepatic glucose output while enhancing glucose uptake into muscle and adipose tissue. Glucose is released through the glucose transporter GLUT2 in the liver, whereas GLUT4 is an insulin-sensitive receptor that mediates glucose uptake in muscle and fat. The major canonical insulin signaling cascade required for this maintenance of systemic blood glucose concentration and hemostasis activates the key protein kinase Akt (Boucher, Kleinridders et al. 2014), known in three isoforms.

The binding of insulin to its receptor protein activates its intrinsic tyrosine-kinase activity, which phosphorylates insulin-receptor substrate (IRS) proteins on tyrosine residues that then serve as anchoring sites for the p85 regulatory subunits of p85/p110 phosphatidylinositol 3-Kinase (PI-3K) at the cell membrane (Boucher, Kleinridders et al. 2014). This generates the phosphatidyl 3,4,5-triphosphate (PtdIns(3,4,5)P<sub>3</sub>) from phosphatidyl 4,5-biphosphate (PtdIns(4,5)P<sub>2</sub>) in the membrane, which facilitates recruitment and interaction between the protein kinases PDK1 and Akt. This, in turn, leads to the phosphorylation on threonine 308 of Akt and thus activation. Additional activation of Akt occurs upon its phosphorylation by a second protein kinase, mTORC2. Therefore, Akt is capable of inhibiting the transcription factor FOXO1, which regulates important enzymes for gluconeogenesis thus suppressing this process. Moreover, by limiting the availability of gluconeogenesis substrates, adipocyte lipolysis is also suppressed (Czech 2017).

As previously discussed, obesity is one of the most critical factors for developing insulin resistance. Metabolism of adipose tissue is dependent on releasing of non-esterified fatty acids (NEFAs) and glycerol, hormones (including leptin and adiponectin) and proinflammatory cytokines (Shoelson, Lee et al. 2006): all these products are increased in obesity.

In obese patient insulin resistance could be induced through a retinol-dependent mechanism by retinol-binding protein-4 (RBP4) an adipokine that reduces phosphatidylinositol-3-OH kinase (PI(3)K) signalling in muscle and enhance the expression of phosphoenolpyruvate carboxykinase (PEPCK), the gluconeogenic enzyme in the liver (Yang, Graham et al. 2005).

Both in obesity and type 2 diabetes have been observed increasing in NEFA levels associated with insulin resistance. It has also been proposed that increased NEFA delivery or decreased intracellular metabolism of fatty acids results in an increase in the intracellular content of fatty acid metabolites such as diacylglycerol (DAG), fatty acyl-coenzyme A (fatty acyl-CoA), and ceramides. These metabolites, in turn, activate a serine/threonine kinase cascade leading to serine/threonine phosphorylation of insulin receptor substrate-1 (IRS-1) and insulin receptor substrate-2 (IRS-2), and a reduced ability of these molecules to activate PI(3)K. Subsequently, events downstream of insulin-receptor signaling are diminished (Shulman 2000).

On the contrary, adiponectin acts on insulin sensitivity by stimulating fatty acid oxidation in an AMP-activated protein kinase (AMPK) and peroxisome proliferator-activated receptor  $\alpha$  (PPAR- $\alpha$ )-dependent manner.

In addition to adipocyte-derived factors, the development of insulin resistance is due to the increase of the release of tumor necrosis factor- $\alpha$  (TNF- $\alpha$ ), interleukin-6 (IL-6), monocyte chemoattractant protein-1 (MCP-1) and additional products of macrophages and other cells that populate adipose tissue (Kadowaki, Yamauchi et al. 2006).

TNF- $\alpha$  and IL-6 act through classical receptor-mediated processes to stimulate both the c-Jun aminoterminal kinase (JNK) and the I $\kappa$ B kinase- $\beta$  (IKK- $\beta$ )/nuclear factor- $\kappa$  (NF- $\kappa$ B) pathways, resulting in upregulation of potential mediators of inflammation that can lead to insulin resistance. Further, other pathways are involved in cytokine-induced insulin sensitivity impairment such as the inducible nitric oxide synthase (iNOS) and suppression of cytokine signaling proteins (SOCS), the latter involved in inhibiting the JAK-STAT signaling pathway (Perreault and Marette 2001). Secretion of these pro-inflammatory proteins, particularly MCP-1 by adipocytes, endothelial cells, and monocytes, increases macrophage recruitment and thus contributes to fueling the process (Weisberg, McCann et al. 2003).

Moreover, as in a vicious circle, hyperglycemia increases the formation of reactive oxygen species (ROS), which promotes the activation of the NLRP3 (NOD-, LRR- and pyrin domain-containing 3) inflammasome and caspase1, thus allowing the production of mature interleukin-1 $\beta$  (IL-1 $\beta$ ).

Recently it has been demonstrated the association between obesity and increased gut leakiness that lead to bacterial products (endotoxins) released that, along with inducing changes to the gut flora, may further trigger tissue inflammation (Ley, Backhed et al. 2005). These stresses trigger several intracellular inflammatory pathways. Indeed, endotoxins, free fatty acids, and other lipids recruit the glycoprotein Fetuin-A, which, together with the recruiting agent, activates TLR2 and TLR4, thereby leading to the NF- $\kappa$ B-mediated release of cytokines and chemokines (Vandanmagsar, Youm et al. 2011).

#### ***1.4 Aging and cellular senescence***

Aging is defined as a progressive loss of physiological integrity that leads to a gradual decline in tissue and organ function and is characterized by an increased risk of disease and death (Lopez-Otin, Blasco et al. 2013).

“Chronological age” is the primary risk factor for several pathologies, including diabetes, cardiovascular disorders, cancer, and neurodegenerative diseases and that are classified for this reason as age-related diseases (ARDs).

Aging derived from a complex interaction among environmental, stochastic, genetic, and epigenetic factors (Franceschi and Campisi 2014).

A chronic, low-grade inflammation termed ‘inflammaging’ is one of the main features of human aging. Inflammaging is a systemic condition in the absence of overt infection (“sterile” inflammation) and it represents a highly significant risk factor for both morbidity and mortality in elderly people, as the majority of ARDs share inflammatory pathogenesis (Franceschi, Bonafe et al. 2000).

Although acute inflammation can be beneficial to counteract harmful conditions such as traumatic tissue injury or invading pathogens, during aging this response may be defective. Many of the features of acute inflammation continue as chronic, but inflammation usually became of low grade and persistent, resulting in responses that lead to tissue degeneration (Franceschi and Campisi 2014).

Cellular senescence is a recognized hallmark of human aging. Indeed, in the elderly, the number of senescent cells increases in multiple tissues and are found to accumulate in the course of age-related pathology (Herbig, Ferreira et al. 2006, Lawless, Wang et al. 2010). In a health and young tissue, senescent cells are usually cleared by the immune system (Kang 2011). However, in aged person, immune functions are impaired, a phenomenon named as immunosenescence, and the clearance of senescent cells are not efficient, thus exacerbating inflammation (Shaw, Joshi et al. 2010).

Recent data on animal models showing that periodic clearance of senescent cells, using genetic systems or drugs, is accompanied by a mean lifespan and healthspan extension, coupled with reduced inflammatory gene expression in multiple tissues, including kidney and heart (Baker et



al, 2011). Moreover, the accumulation of senescent cells has recently been suggested to be a crucial factor contributing to systemic inflammation. Mechanistically, senescent cells likely fuel chronic inflammation because of acquisition of a specific phenotype named “senescence-associated secretory phenotype” (SASP), characterized by the enhanced secretion of pro-inflammatory molecules and mediators (Tchkonia, Zhu et al. 2013). Thus, senescent cells burden can modify the tissue microenvironment in a SASP-mediated manner and these sites are prominent for many age-related pathologies. Clearly, preventing the development of the SASP or ameliorating its effects could mitigate the deleterious effect of senescent cells.

#### **1.4.1 The hallmarks of cellular senescence: focus on telomere shortening**

Senescence is a cellular program that induces a stable growth arrest accompanied by viability, metabolic activity and a distinct phenotypic alteration (Campisi and d'Adda di Fagagna 2007, Kuilman, Michaloglou et al. 2010). For the first time, in 1961 this phenomenon was described by Hayflick in human fibroblasts serially passaged in culture. The non-dividing cells remained viable for many weeks but failed to duplicate despite the presence of space and nutrients in the medium, reaching the so-called “Hayflick limit” (Hayflick and Moorhead 1961).

To date, this process is designated as “cellular senescence” and can be triggered by a plethora of stimuli, including oncogenes activation, telomere shortening or damage, mitochondrial deterioration, oxidative stress, and excessive DNA damage (Baker and Sedivy 2013).

Telomeres are regions of repeat sequences, at the end of each linear chromosome, bound by multiple telomeric proteins. In mammalian cells, telomere DNA contains double-stranded tandem repeats of TTAGGG followed by terminal 3' G-rich single-stranded overhangs.

Telomere DNA probably adopts the T-loop structure, where the telomere end folds back on itself and the 3' G strand overhang invades into the double-stranded DNA (the so-called D-loop).

The functional telomeric structure prevents the degradation or fusion of chromosome ends and thus is essential for maintaining the integrity and stability of eukaryotic genomes. Due to the intrinsic inability of the replication machinery to copy the ends of linear molecules, telomeric DNA is subject to attrition during mitosis and the replication process can go on until a critical threshold of telomere length is reached.

Telomeric DNA is also highly prone to oxidative damage, and the increase in oxidative stress induces its shortening (Rhee, Ghosh et al. 2011). For these reasons, telomeres shortening is a widely used indicator of replicative senescence and cumulative genomic damage in somatic cells (Allsopp, Chang et al. 1995).

Dysfunctional telomeres as well as non-telomeric DNA damage, namely DNA double-strand breaks (DSBs), trigger a classical DNA damage response (DDR), which imposes the cell growth arrest to repair DNA and preserve genome integrity.

In this cascade of process, the MRE11-RAD50-NBS1 (MRN) complex is one of the first factors to directly bind to DSBs, locally triggering the auto-phosphorylation and activation of the ATM kinase (primary recruitment). The activated form of ATM (pATM<sup>S1981</sup>) then phosphorylates the C-terminal portion of histone H2AX ( $\gamma$ H2AX), allowing the recruitment of the DDR mediator factors MDC1 and 53BP1 (TP53BP1) (secondary recruitment). This event functions as a positive feedback loop which amplifies the DDR signal and spreads the accumulation of DDR factors for hundreds of kilobases starting from the DSB. The signal is ultimately transduced from the apical kinase ATM to downstream kinases such as CHK2, thus enforcing checkpoint activation (Gioia, Francia et al. 2019). Both damage- and telomere-initiated senescence depend strongly on the tumor suppressor p53 and are usually accompanied by the expression of the cyclin-dependent kinase inhibitor-1 p21 (Campisi and d'Adda di Fagagna 2007). In addition to p53, replicative senescence is linked to p16INK4A (a cyclin-dependent kinase inhibitor). P16INK4A is encoded, together with ARF, by the INK4a/ARF locus. Indeed, activation of both the p53 and p16INK4A–RB pathways

is essential for the induction of senescence in a variety of human cell types. Thus, the DDR is an evolutionarily conserved signaling cascade, which directs cell fate toward cell cycle progression, senescence or apoptosis.

#### **1.4.2 Senescent cell markers**

Senescent cells display several features which can be detected by multiple techniques. Given the heterogeneity of senescent cells and the lack of specificity of the markers, a combination of different techniques is often used and encouraged for the detection of senescent cells (Hernandez-Segura, Nehme et al. 2018).

- *Cell cycle arrest*: the first method is the measurement of the colony-formation potential or the DNA synthesis rate by BrdU/EdU-incorporation assays, to measure cell proliferation potential. The second includes measuring the expression level of the CDKIs p16 and p21(Sharpless and Sherr 2015).
- *DDR*: the presence of  $\gamma$ -H2AX foci measured by immunostaining demonstrates continuous and unrepaired DNA damage (Sharpless and Sherr 2015).It also can be used the measurement of the phosphorylated p53 level.
- *Secretory phenotype*: immunostaining or ELISA for cytokines (e.g., IL-1a, IL-6, and IL-8), chemokines (e.g., CCL2) and metalloproteinases (e.g., MMP-1 and MMP-3) are used to detect the protein expression and secretion, particularly IL-6 (Coppe, Patil et al. 2008).
- *Apoptosis resistance*: the upregulation of the BCL-proteins Bcl-2, Bcl-w, or Bcl-xL has been used as a marker of senescence (Yosef and Krizhanovsky 2016). However, it is not yet regularly used.
- *Cell size*: in vitro, the enlarged cell body and irregular shape of senescent cells is easily evaluated by regular bright-field microscopy.

- *Increased lysosomal content*: one of the first tests used to assess senescence was the Senescence-Associated  $\beta$ -Galactosidase (SA- $\beta$ -Gal), the most common marker of lysosomal activity (Lee, Han et al. 2006). This marker partly reflects the expansion of the lysosomal compartment, giving rise to an increase in  $\beta$ -gal activity that can be measured also at suboptimal pH 6. Alternatively, Sudan black B (SBB) or its biotin-labeled analog (GL13) can be used to detect lipofuscins from old lysosomes, and Lyso-Trackers or orange acridine can reveal high lysosomal contents (Studencka and Schaber 2017).

### **1.4.3 Senescence-associated secretory phenotype (SASP)**

Cells undergoing senescence display a crucial alteration in their secretome, acquiring a typical senescence-associated secretory phenotype (SASP). The SASP consists of a plethora of factors that includes cytokines (i.e. interleukin (IL)-1 $\alpha$ / $\beta$ , IL-6, IL-8), growth factors (i.e. EGF, FGF, VEGF), proteases (i.e. metalloproteinase MMP-1, -2, and -3) and other non-soluble extracellular matrix proteins (i.e. collagens, fibronectin, laminin). Although a core of pro-inflammatory factors is shared in all type of senescent cells, the specific SASP composition depends on the cell type and on the senescence inducer (Coppe, Desprez et al. 2010). The SASP is a temporally regulated program. In culture, cells develop a full SASP five days later the senescence induction. Not all SASP factors start to be secreted at the same time (Coppe, Patil et al. 2008). Indeed, most of them are released in small amounts until several days after the induction of genotoxic stress. Accordingly, recent studies have shown that a certain number of secreted factors can be expressed much earlier than others and can influence the subsequent expression of other SASP factors (Malaquin, Martinez et al. 2016). Particularly, pro-inflammatory cytokines IL-1 $\alpha$  and IL-1 $\beta$  play a critical role in the early phase of the SASP, as IL-1 $\alpha$  acts as an upstream regulator of IL-6/IL-8 cytokine network. Of note, during senescence, IL-1 $\alpha$  and IL-1 $\beta$  are both secreted at low levels

compared to IL-6 and IL-8, which can act in an autocrine manner to reinforce the senescence growth arrest.

IL-1 $\beta$  originates from its precursor pro-IL1 $\beta$  and it is activated to its mature secreted form after a proteolytic cleavage mediated by a component of the inflammasome complex, the caspase-1 (Gallagher-Beckley, Lan et al. 2013). IL-1 $\alpha$  acts intracellularly or as a cell surface-bound protein.

Beyond the early phase of the SASP, IL-1 $\alpha$  has been implicated in the upregulation of microRNA-146a/b, which are responsible for the inhibition of interleukin-1 receptor-associated kinase 1 (IRAK-1) and the resulting on reduction in IL-6. This mechanism suggests the possibility that a negative feedback loop may restrict the activity of the late mature SASP to prevent pervasive chronic inflammation. Recently other cytokines of the IL-1 family have been discovered: in particular IL-38, considered a potential inhibitor of the IL-1 and Toll-like receptor families. IL-38 exerts anti-inflammatory properties, especially on macrophages, by inhibiting secretion of pro-inflammatory cytokines. (Garraud, Harel et al. 2018).

The SASP program is triggered by a variety of genotoxic senescence-inducing stress (e.g. telomere shortening or damage, cytotoxic drugs, radiation, oncogene activation, oxidative stress) (Coppe, Patil et al. 2008). DNA damage activates DDR, which allows for the recruitment and activation of ATM and subsequent DDR signaling cascade. Importantly, when DNA lesions are irreparable and a DDR signal is persistent, cells activate the senescence program and consequently SASP.

Thus, constant DNA damage activation signaling is required for maintaining senescence-associated inflammatory cytokine secretion. However, it could occur that cells overexpressed the cell-cycle inhibitors (P16/p21) leading to trigger a growth arrest and share an aspect of senescent cells but fail to activate DDR and do not produce SASP (Coppe, Desprez et al. 2010). Notably, although the DDR is important for both the SASP and the senescence-associated growth arrest, the molecular regulation of these two processes is quite different, as p53 plays no role in establishing and maintaining the SASP despite its crucial function in regulating the growth arrest.

Passos *et al.* proposed that persistent DDR triggers the continued production of reactive oxygen species (ROS), forming a dynamic feedback loop that actively maintains a deep senescent state (Passos, Nelson et al. 2010).

However, canonical DDR signaling seems not to be sufficient for the SASP. Another important pathway activated in response to cell stress is the mitogen-activated protein kinase p38 (p38MAPK). P38MAPK phosphorylation is important for the establishment of the senescence growth arrest due to its ability to activate both the p53 and pRb/p16 pathways.

Freund and colleagues showed that p38MAPK activity is necessary and sufficient for the development of a SASP in cells induced to senesce by direct DNA damage or oncogenic RAS. In these contexts, p38MAPK is not activated quickly, but rather with delayed kinetics characteristic of the SASP (Freund et al., 2011).

These different signaling pathways (DDR, p38MAPK and IL-1 pathway) converge toward the activation of the nuclear transcription factor- $\kappa$ B (NF- $\kappa$ B), necessary for the expression of genes encoding SASP factors (Salminen, Kaarniranta et al. 2012) and CCA AT/enhancer-binding protein beta (C/EPB $\beta$ ). Interestingly, these transcription factors were previously known to be involved in the regulation of cellular stress and inflammatory signals by promoting the expression of many cytokines.

Interestingly, the rapamycin, known as an inhibitor of the mTOR pathway, has long been known to extend lifespan and healthspan in mice and also to control SASP protein secretion by enhancing IL-1 $\alpha$  translation. Moreover, the chromatin cytoplasmic sensing by the cGAS/STING pathway has been proposed as a trigger for SASP induction as well. (Dou, Ghosh et al. 2017).

SASP at transcription level can also be dependent on epigenetic changes. Notably, the histone deacetylase sirtuin 1 (SIRT1) is downregulated during senescence and leads to increased expression of IL-6 and IL-8 via histone acetylation of the promoter regions (Hayakawa et al, 2015).

On one side, the effects of the SASP is deleterious: it can transmit cellular senescence on nearby healthy cells, thus representing a non-cell-autonomous mechanism. This paracrine effect could potentially explain persistent chronic inflammation, inflammaging, that contributes to multiple age-related phenotypes (Franceschi and Campisi 2014). In the case of cancer microenvironment, SASP of senescent stromal fibroblasts can sustain tumor growth and invasion and can even promote long-term cancer therapy resistance.

To the contrary, SASP can also have a beneficial role in a variety of processes as is involved in microenvironment modification, immune surveillance activation, and senescent cell cycle arrest reinforcement in an autocrine and paracrine manners. Physiologically, senescent cells play an important beneficial role in embryonic development and in the organization of tissue repair responses that promote wound healing (Demaria, Ohtani et al. 2014). Moreover, SASP can play a critical role in removing the transient senescent cells inducing immune-mediated clearance and modulating the differentiation of neighboring cells. It has been suggested that senescent cells can also promote cellular plasticity and tissue regeneration (Ritschka, Storer et al. 2017) (**fig.7**).

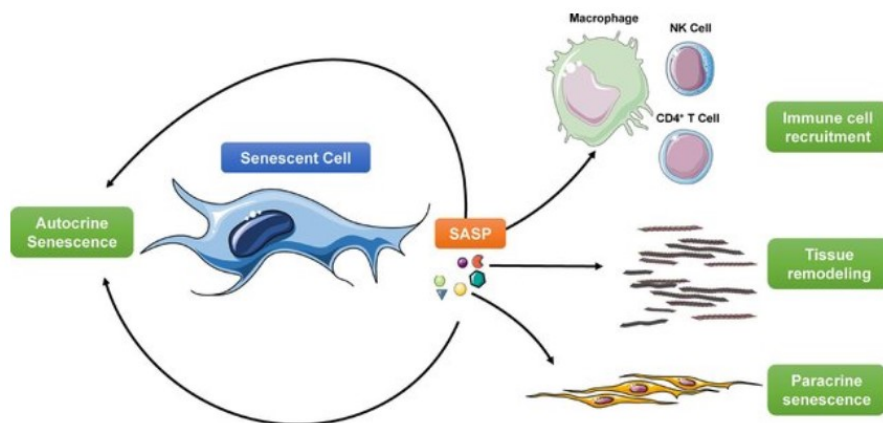


**Figure 7. Functions of the SASP.** The SASP mediates many of the cell-extrinsic functions of senescent cells. Among those it reinforces several aspects of senescence including growth arrest and the SASP itself via an autocrine loop. The SASP also recruits immune cells, remodel the surrounding tissue, inducing angiogenesis and reducing fibrosis. Finally, the SASP spread the senescence phenotype in a paracrine manner to surrounding cells (McHugh and Gil 2018).

## ***2. Aim of the work***

Age-related disorders (ARDs) have become widespread throughout the world and the leading cause of death in developed countries, characterized by chronic, sterile, low-grade inflammation named *inflammaging*.

Obesity is a powerful risk factor for many age-related diseases, such as hypertension, dyslipidemia, cardiovascular complications, impaired glucose tolerance or Type 2 diabetes mellitus (T2DM).

Recently, senescent cells have been found to accumulate in adipose tissue of obese and diabetic humans and mice (Minamino 2009, Villaret, Galitzky et al. 2010, Schafer, White et al. 2016) but it is unclear if their presence is a causal driver. The molecular bases on how obesity accelerates the aging of adipose tissue are only now beginning to come to light.

My PHD thesis focus on the evaluation of the role and the phenotype of macrophages during obesity and obesity-related disease. Our hypothesis was that macrophages recruited within adipose tissue during obesity could eventually become senescence, triggered by obese-related metabolic stimuli such as hyperglycemia. Therefore, in hyperglycemic condition, obese adipose tissue senescent cells foster the inflammatory burden leading to the development of insulin resistance and T2DM.

To assess this hypothesis, we carried out histological analysis of *ex vivo* adipose tissue, *in vitro* analysis by setting a coculture and cytofluorimetric analysis of monocyte subpopulations.

### **- *Histological analysis***

Despite the number of senescent cells is relatively small in human tissues, they have been associated with multiple diseases of aging, emerging as useful therapeutic targets for ARDs. However, it is still unclear which cells *in vivo* carry these markers of senescence. Certainly, the pathogenesis of a plethora of ARDs have been associated with accumulation of macrophages and



more recently, it has been demonstrated that senescent cells have been involved in the same diseases. Fat tissue is mainly distributed into two body compartments with different metabolic characteristics: subcutaneous adipose tissue (SAT) and visceral adipose tissue (VAT). A particular attention has been directed to visceral adiposity owing to its association with various medical pathologies, including ARDs (Shuster, Patlas et al. 2012).

Thus, our first aim was to detect senescent macrophages within adipose tissue of obese individual, particularly observing the differences between VAT and SAT. To do this, we recruited 17 obese patients ( $BMI \geq 38 \text{ kg/m}^2$ ) from the Obesity Clinic of Ospedali Riuniti of Ancona and we collected abdominal VAT and SAT during bariatric surgery. Then, we develop a method which would allow us to detect a double staining in the adipose tissue: SA- $\beta$ -Gal activity and the pan macrophage marker CD68.

- **In vitro analysis**

Adipose tissue macrophages (ATMs) have been recognized as important elements in immune function and inflammation (Weisberg, McCann et al. 2003). However, in human the different ATM phenotypes and the polarization mechanisms remain still to deepen.

Two different phenotypes of ATMs have been already well-characterized: classically activated pro-inflammatory ATMs (M1) and alternatively activated anti-inflammatory ATMs (M2), wherein M1 show a pro-inflammatory phenotype, whereas M2 exhibit anti-inflammatory features. Obesity-induced insulin resistance is a key component in the pathogenesis of T2DM and it is known that ATMs accumulation in obese adipose tissue is involved in the disease development. Hyperglycemia is the major hallmark of T2DM, and it is associated with a range of complication. New exciting papers have demonstrated that high glucose could induce a senescence phenotype in different cellular type *in vitro* and even in *in vivo* studies (Kitada, Nakano et al. 2014, Prattichizzo, De Nigris et al. 2018, Zhang, Wang et al. 2019)

Thus, the second aim of this thesis was to decipher the effect of hyperglycemia on macrophage polarization and to characterize the senescent induced phenotype of these cells, compared to M1 and M2 condition, and naïve M0 (as control). Moreover, we want to evaluate the interaction between macrophages and adipocytes by taking advantage of coculture assays, and particularly the effect of the adipose cells on hyperglycemia-induced senescent macrophages.

- **Cytofluorimetric analysis**

Obesity is recognized as a low-grade inflammatory disease, that lead to the development of metabolic and cardiovascular complications. The systemic inflammation results, at least in part, from activation of circulating immune cells, vascular endothelium, and excessive accumulation of inflammatory cells in adipose tissue. Monocytes, acting critically in inflammatory diseases, have been recently categorized in three subsets according to the expression of LPS (CD14) and the FcγRIII (CD16) receptors (Devevre, Renovato-Martins et al. 2015).

Classical monocytes (CD14<sup>++</sup>CD16<sup>-</sup>) represent approximately 80% of the total population, whereas monocytes expressing CD16, which account for about 20%, have been further classified into two subtypes: non-classical (CD14<sup>++</sup>CD16<sup>+</sup>) and intermediate (CD14<sup>low</sup>CD16<sup>+</sup>) monocytes (Costantini, Viola et al. 2018).

Recent papers described an increased proportion of circulating non-classical and intermediate subsets in human chronic pathologies associated with low-grade inflammation, including obesity as well as decrease in proportion of these two subsets during weight loss (Devevre, Renovato-Martins et al. 2015). Moreover, M1/M2 profiles have also been examined in circulating monocytes, both in physiological and pathological conditions. Analysis of monocytes from patients affected by ARDs has led to the observation of a significant association between CD163<sup>+</sup> monocytes and diabetes and its complications (Kawarabayashi, Motoyama et al. 2017).

In this framework, the third goal of this thesis was the evaluation of the three monocyte subsets in obesity-related morbidity, particularly acute myocardial infarction, compared to a healthy group. Further, we wanted to investigate the M1/M2 profile within monocyte subsets by cytofluorimetric analysis of CD80/CD163 marker expression.

Finally, based on a paper published in Nature Protocols (Debacq-Chainiaux, Erusalimsky et al. 2009), we set up a cytofluorimetric analysis of SA- $\beta$ -Gal activity in M1/M2 monocyte subsets of elderly patients. This preliminary study aimed to identify which subpopulations among circulating monocytes show a significant senescent status.

The hypothesis that progressive up-regulation of inflammatory gene expression and high levels of inflammatory signaling facilitate the development and progression of the major age-related diseases (ARDs), such as cardiovascular disease (CVD), type 2 diabetes mellitus (T2DM) and Alzheimer Disease (AD), is continuously supported by abundant data. Thus, the identification of circulating biomarker is fundamental to improve the diagnosis and/or prognosis of these major ARDs.

Particularly, patients suffering from such diseases show subclinical/clinical inflammation and, interestingly, deregulation of most circulating *inflammation-miRs* (Wang, Zhang et al. 2010).

MiRNAs are short-non coding RNA sequence that play a significant role in gene regulation acting as repressors as well as activators, mainly at the post-transcriptional level (Breving and Esquela-Kerscher 2010). A mounting body of evidence has been documenting a relatively small number of miRNAs that are involved in regulating inflammation: their prototypes are miR-155, miR-21, and miR-146a (Quinn and O'Neill 2011), namely the *inflammation-miRs* (Olivieri, Rippo et al. 2013).

One aim of this second part of my PhD thesis was to disentangle the complex relationship between age, hyperglycemia, and miR-146a circulating levels. To do this we investigated the levels of miR-146a plasma levels in healthy subjects and in T2DM patients at different ages and in both genders.

Furthermore, we considered even another important marker of aging, the senescence associated- $\beta$ -Galactosidase activity. In particular we wanted to detect the level of activity in plasma, as few recent evidence showed an altered plasmatic  $\beta$ -Gal activity in patients affected by some ARDs. The aim was to investigate if plasmatic  $\beta$ -Gal activity is modulated in T2DM patients and if the age could affect such modulation.

Moreover, the identification of diagnostic-prognostic biomarkers of dementia has become a global priority due to the prevalence of neurodegenerative diseases in aging populations.

The second aim of this section of the thesis was to assess the diagnostic performance of cerebrospinal fluid (CSF) biomarkers across patients affected by either Alzheimer's disease (AD), tauopathies other than AD (TP), or vascular dementia (VD), and cognitively normal subjects (CNS). One hundred fifty-three patients were recruited and tested for classical AD CSF biomarkers- Amyloid- $\beta$ 42 and tau proteins - and novel candidate biomarkers - microRNA (miR) -21, -125b, -146a, and -222 and neurofilament (NF-) light.

### ***3. Materials and methods***

#### ***3.1 Patients***

For histological analysis we recruited 17 obese patients ( $\text{BMI} \geq 38 \text{ kg/m}^2$ ) from the Obesity Clinic of Ospedali Riuniti of Ancona and we collected abdominal visceral (VAT) and subcutaneous (SAT) adipose tissue during bariatric surgery. The study protocol was approved by the Ethics Committee of Ospedali Riuniti (Ancona, Italy). Obesity was diagnosed according to the criteria. Subjects on anti-inflammatory drugs were excluded from the study. The information collected included anthropometric data and medical history.

For monocyte subsets analysis by flow cytometer, 31 healthy subjects and 21 AMI patients were enrolled at the Ancona National Institute for Health Care of the Elderly (INRCA) in the framework of an Italian national study directed at identifying the biological parameters associated with healthy/unhealthy aging. The study protocol was approved by the INRCA ethics board. Participants signed an informed consent before enrolment. Healthy subjects were further divided in two subgroups, younger ( $n=12$ ) and older ( $n=19$ ), according to age ( $<65$  years and  $\geq 65$  years), in order to obtain two study groups that were statistically homogeneous and comparable.

For  $\beta$ -Gal analysis by flow cytometer, we recruited 21 patients from the Italian National Research Center on Aging (INRCA-IRCCS) of Ancona and we collected blood sample. Inclusion criteria were: age  $\geq 75$ , absence of infectious or autoimmune diseases, cancer, neurodegenerative disorders. Subjects with type 2 diabetes were included only if they had proper glycemic control ( $\text{HbA1c} < 7\%$  and fasting glucose  $< 126 \text{ mg/dL}$ ).

For the evaluation of the circulating miR-146a, 188 healthy subjects (CTRs) and 144 T2DM patients were recruited from INRCA-IRCCS, Ancona. The Institutional Review Board of INRCA approved the study protocol and all enrolled subjects provided a written informed consent.

We considered 153 subjects consecutively admitted to the Neurology Unit of INRCA-IRCCS, of Ancona. Participants with CSF sample available were included in the study. The Institutional Review Board of INRCA approved the study protocol and all study participants, or their next of kin, provided written informed consent in the case of relevant cognitive impairment. All recruited subjects were between 38 and 90 years of age.

Based on the cognitive assessments and clinical diagnosis, the patients were grouped into the following diagnostic categories: 70 AD, 23 TP, 17 VD and 43 defined as cognitively normal subjects (CNS). The TP group was composed of: 3 patients with progressive supranuclear palsy (PSP), 19 patients with frontotemporal dementia (FTD) and 3 patients with corticobasal degeneration (CBD). Tauopathies and vascular dementia are classified as Non-Alzheimer disease (NAD).

### ***3.2 SA- $\beta$ -Galactosidase staining for fresh organ***

Tissues to be staining and embedded should be cut to a size no larger than 3-5mm thick. Tissue should be washed once with PBS 1x for 1 minute and then fixed with a Fixative Solution provided by the senescence detection kit (Biovision) for 1 hour. After washing again with PBS 1x for 1 minute, tissue was stained with Staining Solution provided by Senescence detection kit (Biovision), adding a volume to cover the tissue. The staining solution is prepared following the Biovision Protocol (X-Gal substrate: 20 mg/ml). Tissue was incubated at 37 °C (without CO<sub>2</sub>) for 20-22 hours.

### ***3.3 Paraffin embedding***

Tissues to be embedded must be fixed in 4% paraformaldehyde at 4 °C O/N and subsequently rinsed with PBS for 30 min (3 times for 10 min each). All traces of water must be removed (dehydration) because water and paraffin are immiscible. The blocks are transferred sequentially to 70%, 95%, and 100% alcohols for about two hours each (2 times for 50 min each). For paraffin embedding, the tissues need to be cleared with xylol for about two hours (twice for 50 min). Then the blocks were moved in paraffin in an oven at 56°C - 58°C (the melting temperature of paraffin) O/N. The second day, tissues were transferred to a second pot of melted paraffin in the oven for an additional two-three hours.

### ***3.4 Counting of $\beta$ -Gal+ cells in tissue sections***

Paraffin blocks were sectioned at the desired thickness of 4  $\mu$ m on a microtome and floated on a 38°C water bath containing distilled water. Then sections were transferred onto a permanent positive charge coated slide (Superfrost Plus, Menzel-Glaser). The slides were dried overnight. To deparaffinize slides, xylene was used for 5 minutes each. Slides hydration was performed by transferring slides twice for 5 minutes each through 100% alcohol, once through 95% alcohol for 5 minutes and once through 70% alcohol. Tissues were counterstained with Fast Red (Sigma-Aldrich) for 6 minutes and then washed 1 minutes with running water. Dehydrate through one change of alcohol 70%, 95%, 100% and clear in 2 changes of xylene and coverslip using mounting solution. B-Gal+ cells were counted by optical microscopy in the entire section and the tissue area was measured by Image J software. The number of  $\beta$ -Gal+ cells were defined as ratio between total number of positive cells and section area.

### ***3.5 IHC for CD68***

Paraffin blocks were sectioned at the desired thickness of 4  $\mu$ m on a microtome and floated on a 38°C water bath containing distilled water. Then sections were transferred onto a permanent

positive charge coated slide (Superfrost Plus, Menzel-Glaser). The slides were dried overnight, then deparaffinized and hydrated as described in the above section. We blocked endogenous peroxidase activity by incubating sections in 0.3% H<sub>2</sub>O<sub>2</sub> solution in methanol for 10 minutes.

Before immunohistochemical staining of formaldehyde-fixed paraffin-embedded tissue sections, antigen retrieval is used for antigen unmasking. We placed slides in a glass slide holder in a rack and fill with 10 mM Sodium Citrate, then incubated for 20 minutes at 94°C in a water bath and let cool slides for 20 minutes.

Non-specific binding was blocked by incubating with blocking buffer (horse serum) for 60 min at room temperature in a humidified chamber.

CD68 primary antibody (Dako, Denmark) was diluted (1:200) and incubate O/N at 4°C in a humidified chamber. After rinsed for 3 changes in PBS, the anti-mouse secondary antibody was diluted (1:200) and incubated for 30 minutes at room temperature. Vectastain ABC kit (Vector) was applied onto the sections for 1 hour following the instruction.

DAB solution was diluted according to the manufacturer and applied for 3 minutes on the sections or until the desired color intensity is reached. The reaction was stopped by washing with running water. Counterstained was conducted with Fast red stain for 6 minutes and then washed with running water.

Dehydrate through one change of alcohol 70%, 95%, 100% and clear in 2 changes of xylene and coverslip using mounting solution.

### ***3.6 THP-1 culture***

Human monocytic THP-1 cells were purchased from ATCC (Rockville, MD, USA) and maintained in RPMI-1640 medium supplemented with 2-mercaptoethanol to a final concentration of 0.05 mM and with 10 % heat-inactivated fetal bovine serum, 1 % penicillin/streptomycin, and 1 % L-glutamine (all from Euroclone, Milano, Italy).



### ***3.7 Macrophage polarization and hyperglycemia treatment***

To induce polarization of THP1 cells into the M0 phenotype macrophages, PMA (phorbol 12-myristate 13-acetate) was used at a concentration of 100 ng /ml (1 mg/ml stock solution) for 24 hours. Afterwards, we proceeded to polarize M0 macrophages into the M1 phenotype (pro-inflammatory) by adding LPS (15 ng / ml) in RPMI 10% FBS for 48 h, whereas the M2 phenotype (anti-inflammatory) has been induced with IL-4 (25 ng / ml) and IL-13 ( 25 ng / ml) in RPMI 10% FBS for 48 h. THP1 cells were maintained in high glucose medium (60 mM) for 1 week and then treated with 100ng/ml PMA for 24h, in order to obtain the hyperglycemia-induced senescent macrophages (HgSM).

### ***3.8 hMADS differentiation***

hMADS cells grown in low-glucose (1 g/l) proliferation medium [Dulbecco's modified Eagle's medium (DMEM)] supplemented with 10%fetal bovine serum and 2.5 ng/ml hFGF-2 were used between the 16th and the 19th passage. To induce adipose differentiation, they were seeded in proliferation medium on multi-well plates at a density of 4,500 cells/cm<sup>2</sup>. When they reached confluence hFGF-2 was not replaced. The next day (day 0), cells were incubated in adipogenic medium (serum-free proliferation medium/Ham's F-12 medium) containing 10µg/ml transferrin, 5µg/ml insulin, 0.2 nM triiodothyronine, 100µM 3-isobutyl- 1-methylxanthine (IBMX), 1µM dexamethasone, and 100 nM rosiglitazone. Dexamethasone and IBMX were not replaced from day 3 and rosiglitazone from day 9. Cell lipid content was assessed at different time points by Oil Red O staining, whereas differentiation by RT-PCR.

### ***3.9 Trans-well co-culture assay***

THP-1 cells were grown in suspension in RPMI/FCS media, and activation is performed once plated into transwell inserts (Thermo Fisher scientific). THP1 cells were differentiated into M0, M1, M2, and HgSM activated macrophages as described above.

After differentiation, the inserts were washed in RPMI three times before being placed in wells with adipocyte differentiated from hMADS. Co-culture experiments were carried on for 48h so that both cell populations were exposed to the same conditions.

RNA or protein lysates can be obtained from the adipocyte at the bottom of the wells, besides the macrophages can be lysed separately by isolating the insert.

### ***3.10 SA- $\beta$ -Galactosidase staining for cell culture***

Senescence-associated expression of  $\beta$ -galactosidase (SA- $\beta$ -Gal) activity was detected by using Senescence Detection Kit (Catalog #K320 - BioVision Inc., Milpitas, CA, USA). Briefly, Thp-1 cultured in 12-wells plates were fixed for 15 minutes at room temperature and then washed twice in phosphate-buffered saline (PBS). Cells were incubated overnight at 37°C with Staining Solution Mix (containing X-gal).

### ***3.11 Cytokine production***

Culture supernatants were collected at the end of each incubation, centrifuged, and stored at -80°C until use in the assays. IL-6 and IL-38 concentrations (pg/ml) were measured using a commercially available, high-sensitivity ELISA kit (Cayman Chemical and Finetest).

### ***3.12 RNA isolation from adipose tissue and cell culture***

Total RNA was isolated using the Norgen Biotek Kit (#37500, Thorold, ON, Canada), according to the manufacturer's instructions. RNA was stored at -80 °C until use.

For adipose tissue, the first step of extraction with Trizol (ThermoFisher Scientific) and chloroform (Sigma-Aldrich) was performed to isolate and remove lipid droplets.

### ***3.13 Quantitative RT-PCR of mature miRNAs***

MiRNAs expression was quantified by quantitative real-time PCR (RT-qPCR) using TaqMan miRNA assay (Catalog #4427012 - ThermoFisher Scientific), according to the manufacturer's protocol. Briefly, miRNA was reverse transcribed with the TaqMan MicroRNA reverse transcription kit (4366596 – ThermoFisher Scientific), using a miR specific stem-loop primer.

10  $\mu$ l of RT mix contained 2  $\mu$ l of each miR-specific stem-loop primer, 3.34  $\mu$ l of input RNA, 1  $\mu$ l of 10 mM dNTPs, 0.67  $\mu$ l of reverse transcriptase, 1  $\mu$ l of 10 $\times$  buffer, 1.26  $\mu$ l of RNase inhibitor diluted 1:10, and 0.73  $\mu$ l of H<sub>2</sub>O. The mixture was incubated at 16 °C for 30 min, at 42 °C for 30 min, and at 85 °C for 5 min. The 10  $\mu$ l RT-PCR reaction mix included 0.5  $\mu$ l 20x TaqMan MicroRNA Assay, which contained the PCR primers and probes (5'-FAM), 5  $\mu$ l 2x TaqMan Universal Master mix no UNG (4440040 –ThermoFisher Scientific), and 2.66  $\mu$ l RT product. The reaction presented an initial step at 95 °C for 2 min, followed by 40 cycles of 95 °C for 15 sec and 60 °C for 1 min. Data were analyzed with Rotor Gene Q (Qiagen, Hilden, Germany) with the automatic comparative threshold (Ct) setting for adapting baseline. qRT-PCR data were standardized to RNU44. The  $2^{-\Delta Ct}$  method was used to determine miRNA expression.

### ***3.14 Quantitative RT-PCR of mRNA***

RNA amount was determined by spectrophotometric quantification with Nanodrop ONE (NanoDrop Technologies, Wilmington, DE, USA). Total RNA was reverse-transcribed using PrimeScript RT reagent Kit (Takara) according to the manufacturer's instructions. qRT-PCR was performed in a Rotor-Gene Q (Qiagen) using TB Green Premix Ex Taq (Takara) in a 10  $\mu$ l reaction volume. Cycling conditions were: 95 °C for 2 min, and 95 °C for 10 s, 60 °C for 30 s, and 72 °C for 30 s (40 cycles). Samples were run in duplicate. mRNA quantification was assessed using the  $2^{-\Delta\Delta Ct}$  method. Gapdh and Beta-actin were used as an endogenous control.

	<b>FORWARD</b>	<b>REVERSE</b>
TNF $\alpha$	AAGCCTGTAGCCCACGTGTA	GGCACCCTAGTTGGTGGTCTTTG
IL8	GGACAAGAGCCAGGAAGAAA	CCTACAACAGACCCACACAATA
IL6	TGCAATAACCACCCCTGACC	GTGCCCATGCTACATTTGCC
IL-1 $\beta$	AGATGATAAGCCCACTCTACAG	ACATTCAGCACAGGACTCTC
MCPI	GGCTGAGACTAACCCAGAAAAG	GGGTAGAACTGTGGTTCAAGAG
SIRT1	TGTTTCCTGTGGGATACCTGA	TGAAGAATGGTCTTGGGTCTTT
TGF- $\beta$	CCCAGCATCTGCAAAGCTC	GTCAATGTACAGCTGCCGCA
ADIPOQ	GAGATGGACGGACGGAGTCCTTTAGG	CTGGTCATGTTTGTGAAGCTCCC
p21	CCATCCCTCCCCAGTTCATT	AAGACAACACTCCCAGCCC
CD206	TATGGAATAAAGACCCGCTGAC	TGCTCATGTATCTCTGTGATGCT
$\beta$ -actin	TGAGAGGGAAATCGTGCGTG	TGCTTGCTGATCCACATCTGC
GAPDH	GGCACAGTCAAGGCTGAGAATG	ATGGTGGTGAAGACGCCAGTA

**Table 1.** The primers used for qRT-PCR.

### ***3.15 DNA isolation***

DNA was isolated using E.Z.N.A. Tissue DNA Kit Kit (#D3396-01, Omega bio-tek), according to the manufacturer's instructions. DNA was stored at  $-80^{\circ}\text{C}$  until use.

### ***3.16 Telomere length measurement***

The abundance of telomere signal per genome measured by qPCR represents the average telomere length in a given DNA sample.

The amount of input genomic DNA is quantified by measuring the qPCR product of a single copy gene (S) that is used to normalize the signal from the telomere (T) reaction. The single-copy gene is the 36B4, which encodes acidic ribosomal phosphoprotein PO. The resulting T/S ratio represents the average telomere length per genome.

### ***3.17 Protein extraction and immunoblotting***

Cells were washed twice in cold phosphate buffer saline (PBS). Total protein was extracted using RIPA buffer (150 mM NaCl, 10 mM Tris, pH 7.2, 0.1 % SDS, 1.0 % Triton X-100, 5 mM EDTA, pH 8.0) containing a protease inhibitor cocktail (Roche Applied Science, Indianapolis, IN, USA). Protein concentration was determined using Bradford Reagent (Sigma-Aldrich, Milano, Italy). Total protein extracts (20-15 µg) were separated by 10 % or 15% SDS-PAGE and transferred to nitrocellulose membranes (0.45 µm and 0.22 µm) (Bio-Rad, Hercules, CA, USA). Membranes were incubated overnight with primary anti-Sirt1 antibody diluted 1:1000 (Cell Signaling Technology, Beverly, MA, USA), anti-caspase1 antibody diluted 1:200 (Santa Cruz Biotechnology, Santa Cruz, CA, USA), anti-IL-1β antibody diluted 1:1000 (Cell Signaling Technology, Beverly, MA, USA), anti-IKBα antibody diluted 1:1000 (Cell Signaling Technology, Beverly, MA, USA), anti-p21 antibody diluted 1:1000 (Cell Signaling Technology, Beverly, MA, USA) ; subsequently they were incubated with a secondary antibody conjugated to horseradish peroxidase (Vector) for 1 h at room temperature. Immunoreactive proteins were visualized using ECL Plus chemiluminescence substrate (GE Healthcare, Pittsburgh, PA, USA). Membranes were incubated with anti β-actin diluted 1:10,000 (Santa Cruz Biotechnology, Santa Cruz, CA, USA) as an endogenous control. Densitometric analysis were performed with ImageJ software.

### ***3.18 Flow cytometer analysis***

Peripheral venous blood was collected into EDTA coated tubes (Venoject, Terumo Europe NV, Leuven, Belgium). Whole blood samples were placed into EDTA-containing tubes. Six-color flow cytometric analysis was performed with Facs Canto II (Becton- Dickinson, Franklin Lakes, NJ) after labeling 100 µl of blood with the following conjugated monoclonal antibodies: CD14\* allophycocyanin (APC), CD16\* fluorescein isothiocyanate-cyanine 7 (APC-Cy7), CD80\* phycoerythrin-cyanine 7 (PE-Cy7), CD163\* phycoerythrin (PE) (all from Becton-Dickinson).

Cells were incubated for 30 min at room temperature with the optimal dilution of each antibody, according to the manufacturer's instructions. The frequencies of the different subpopulations were calculated using FACS Diva software (Becton-Dickinson). At least 200,000 (monocyte typing) were acquired.

### ***3.19 Fluorescence detection of SA- $\beta$ -Gal activity***

In this procedure, the internal pH of lysosomes is increased to ~pH 6 using lysosomal inhibitory drugs such as chloroquine or bafilomycin A1. Cells are incubated with 5-dodecanoylaminofluorescein di- $\beta$ -D-galactopyranoside (C12FDG), a  $\beta$ -galactosidase substrate that becomes fluorescent (fluorescence acquired in FITC) after cleavage by the enzyme. This procedure can be done using living cells, and SA- $\beta$ -gal positive cells can be detected and quantified by flow cytometry.

### ***3.20 Statistical analysis***

Summarized data are shown as mean  $\pm$  SD or as frequency (%). Independent sample T test was used for the analysis of real-time and densitometric data. Paired T-test was used to compare VAT and SAT. Partial correlation, adjusted for age and BMI, was used to test for correlations in the obese group. For cytofluorimetric analysis, comparisons among groups were performed with univariate or multivariate analysis of variance (respectively ANOVA and MANOVA), as appropriate. Correlations between parameters were calculated using Spearman's rho. Chi square test was used as appropriate. For SA- $\beta$ -Gal activity, mean  $\pm$ SEM was reported and comparison among groups were assessed by Paired T-test.

Data analysis was performed using IBM SPSS Statistics for Windows, version 25 (IBM Corp, Armonk, NY, USA). Statistical significance was defined as a two-tailed p value  $< 0.05$ .

## 4. Results

### 4.1 Histological analysis

#### 4.1.1 Accumulation of SA- $\beta$ -Gal<sup>+</sup> cells in obese abdominal VAT

To investigate the role of senescence in adipose tissue (AT) of obese subjects, SA- $\beta$ -Gal activity assay was performed in abdominal visceral (VAT) and subcutaneous (SAT) adipose tissue of obese individuals underwent bariatric surgery (n=17). SA- $\beta$ -Gal positive (blue) cells (**fig. 8A-B**) in SAT and VAT were counted by optical microscopy and the sections area were measured by ImageJ software. A significant higher number of SA- $\beta$ -Gal positive cells were observed in VAT compared to SAT ( $p < 0.001$ , n=17) (**Fig.8C**).

Subsequently, to evaluate the inflammation burden of total VAT and SAT, we measured the expression levels of three *inflammamirs*, such as miR-146a, miR-21 and miR-155.

We observed a significant elevated level of miR-146a in VAT compared to SAT ( $p = 0.033$ , n=6) and an increasing trend in the expression of miR-21 and miR-155 in VAT compared with SAT (**fig.8D**).

Thus, we confirmed that VAT is characterized by inflammation burden and accumulation of senescent cells in obese individuals.

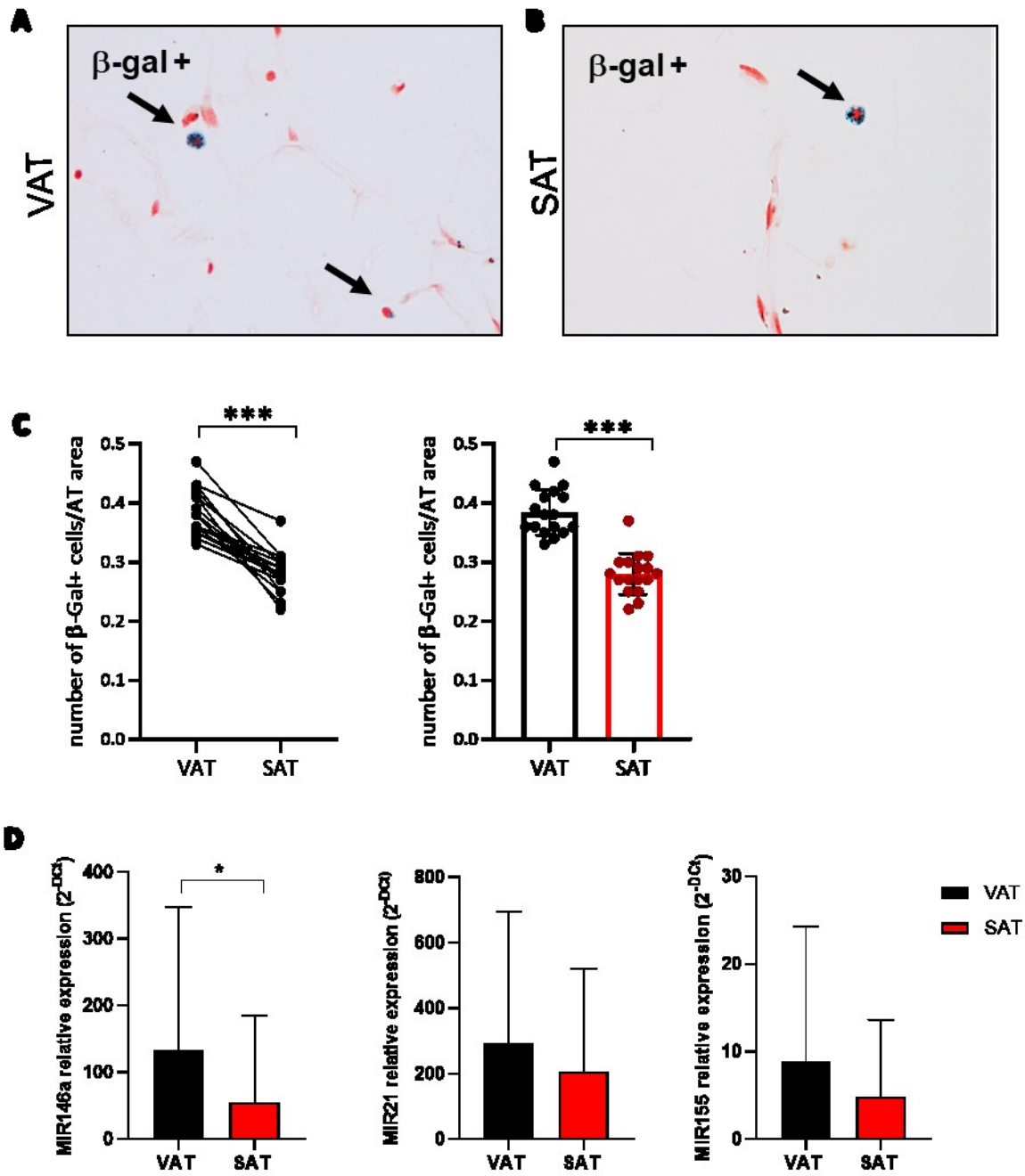


**Figure 8. SA-  $\beta$ -Gal+ cells in adipose tissue.** **A.** histological analysis of visceral and **B.** subcutaneous adipose tissue of obese. **C.** counting of SA-  $\beta$ -Gal+ cells number in VAT and SAT. **D.** miR-146a, miR-21 and miR-155 expression in VAT compared to SAT. \* $p < 0.05$ ; \*\*\* $p < 0.001$ .



#### 4.1.2 Senescent cells in adipose tissue are positive for CD68 pan-macrophage marker

To identify the phenotype of the SA- $\beta$ -Gal<sup>+</sup> cells, abdominal VAT and SAT were stained for CD68, a pan-macrophage marker. Immunohistochemical analysis revealed that the majority of senescent cells (SCs) were positive for CD68 (**Fig. 9A-B**). Moreover, the number of SCs was positively correlated with BMI in VAT ( $r=0.89$ ,  $p < 0.001$ ) but not in SAT samples, whereas in SAT samples SCs number was positively correlated with age ( $r=0.52$ ,  $p=0.029$ ) (**Fig. 9C-D**). These findings suggest a possible involvement of the senescent macrophages of visceral adiposity in obesity-related adipose tissue aging.

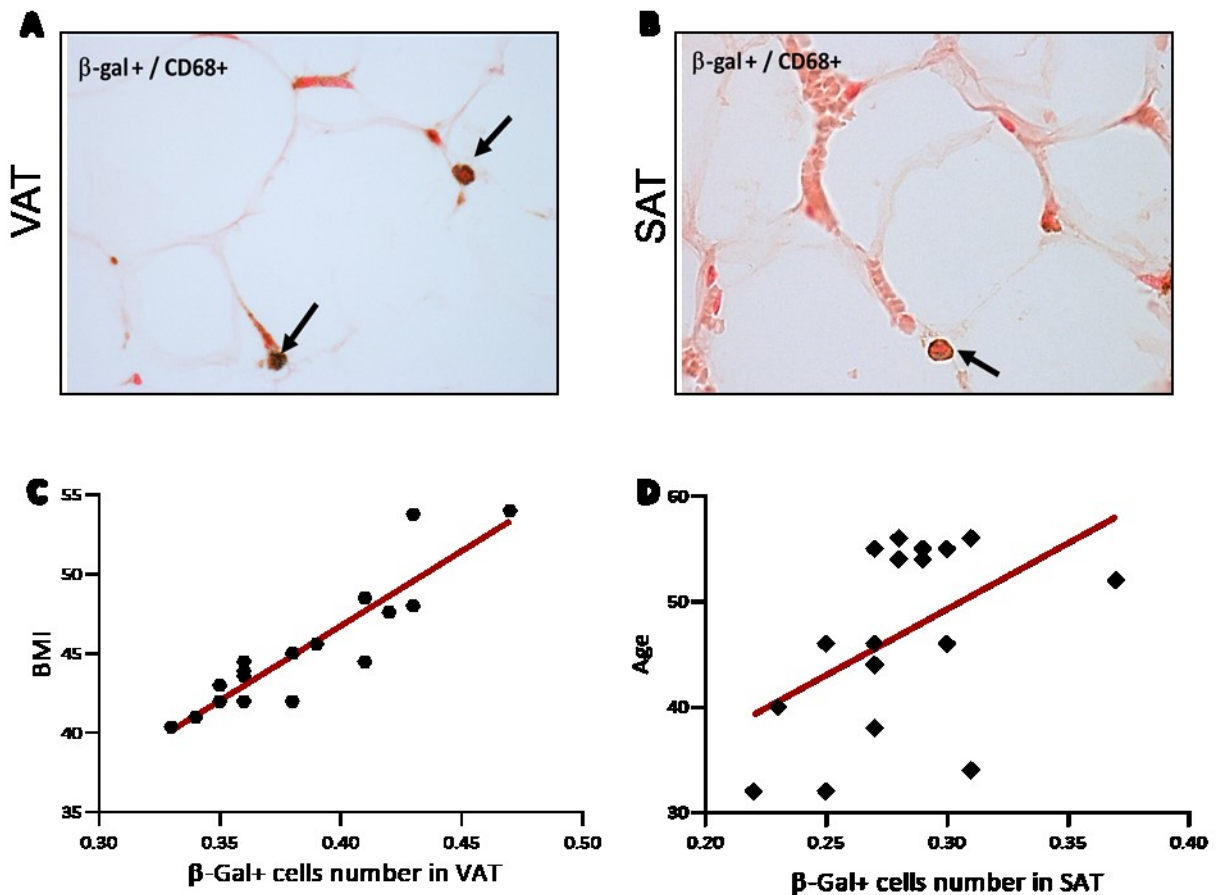


**Figure 9. Senescent macrophages in obese adipose tissue.** A. immunohistochemical analysis of CD68<sup>+</sup> / SA- $\beta$ -Gal<sup>+</sup> cells in VAT and B. SAT of obese individuals. C. correlation between number of SA- $\beta$ -Gal<sup>+</sup> cells and BMI in VAT ( $r=0.89$ ,  $p < 0.001$ ). D. correlation between number of SA- $\beta$ -Gal<sup>+</sup> cells and age in SAT ( $r=0.52$ ,  $p=0.029$ ).

## 4.2 *In vitro* analysis

### 4.2.1 Hyperglycemia triggers a mixed M1/M2 polarization in PMA-induced macrophages

In order to deciphering the role of senescent macrophages within adipose tissue, we focused on characterization of macrophages differentiated from THP1 cells.

THP1 cells were differentiated into naïve (M0) macrophages by PMA to obtain the control condition, then polarized into M1 (by LPS) and M2 (by IL-4 and IL-13) macrophages. In addition, THP1 cells were cultured with high glucose (60mM) medium for one week and then induced with PMA to macrophages, henceforth named hyperglycemia-induced senescent macrophages (HgSM). Morphological features of the different phenotypes were observed by optical microscopy (**fig. 10A**).

ELISA tests showed that HgSMs released significantly low concentration of the cytokines IL-6 ( $p=0.03$ ,  $n=3$ ) and IL-38 ( $p=0.001$ ,  $n=3$ ) compared to M0 condition, whereas cytokines level is significantly elevated in M1 (IL-6,  $p\leq 0.001$ ; IL-38,  $p<0.05$ ), in comparison with control (**fig. 10B**).

Further, miRNA expression analysis revealed that miR-21 level was significantly reduced in HgSMs compared to control (M0). On the contrary, miR-146a expression showed a significant increment in relation to M0, underlining the pro-inflammatory status of M1 (**fig. 10C**).

Moreover, HgSMs showed a significant increased mRNA expression of IL-10 and TNF- $\alpha$  together with a reduced expression of IL-1 $\beta$ , IL-6 and IL-8 cytokines as well as the M2 marker CD206 and p21, compared to M0. M1 exhibited significant high expression of TNF- $\alpha$ , IL-6 and IL-8, whereas CD206 is significantly elevated in M2 in relation to control (**fig.10D**).

Notably, data suggested that hyperglycemia trigger a polarization toward a mixed M1/M2-like phenotype.

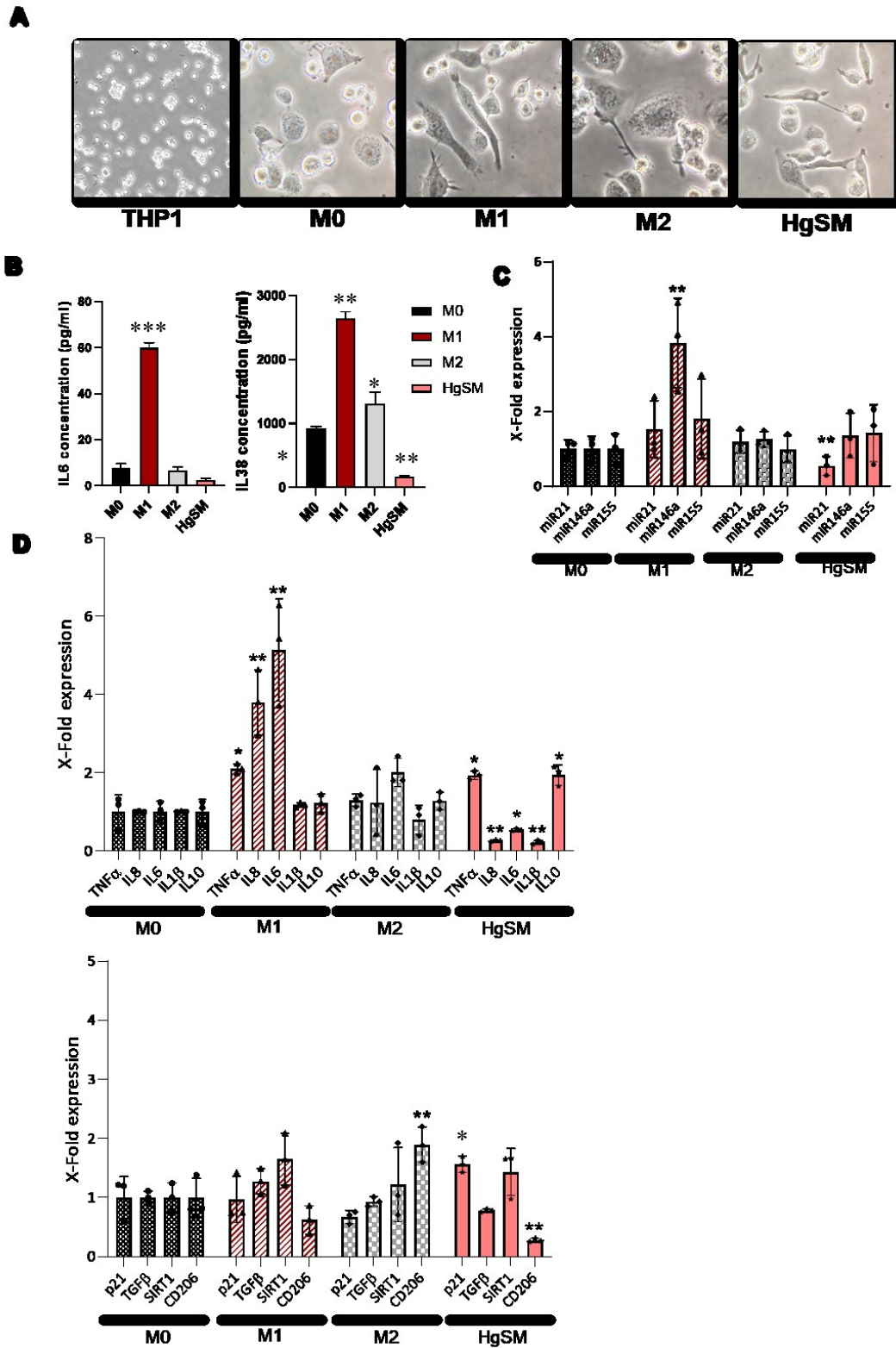


**Figure 10. Analysis of PMA-induced macrophage phenotypes.** A. THP1 cells and M0, M1, M2 and HgSM polarization observed by optical microscopy. B. IL-6 and IL-38 concentration (pg/ml) measured by ELISA. C. miRNA expression analysis by RT-PCR. D. mRNA expression analysis by RT-PCR. \* $p \leq 0.05$ ; \*\* $p \leq 0.01$ ; \*\*\* $p \leq 0.001$

#### **4.2.2 HgSMs show features of senescent cells**

Further, the replicative capability and a number of senescence biomarkers were analysed in THP1 cells cultured in hyperglycemic condition to establish if they acquire a senescent phenotype.

Proliferative activity of THP1 cells was quantified in normoglycemic (11mM of glucose) and hyperglycemic (60mM of glucose) conditions. No significant difference in the rate of proliferation was observed in the two different conditions (**fig. 11A**).

SA-  $\beta$ -Gal activity was significantly higher in HgSMs than in M0 macrophages, as shown by the quantitative analysis carried out with optical microscopy (**fig. 11B**). Strikingly, monocyte to macrophage differentiation induced the acquisition of SA  $\beta$ -gal positivity in a subset of cells but hyperglycemia significantly strengthened this effect.

Of note, the assessment of telomere length demonstrated a significant shortening of telomeres by half in HgSMs compared to control and even M1 and M2 macrophages (**fig. 11C**).

Finally, according to data shown above, protein levels measured by western blot analysis seem to reflect the mixed M1/M2 phenotype. IKB- $\alpha$  was significantly reduced in HgSM, even if caspase-1 and IL-1 $\beta$  were reduced compared to M0 macrophages (**fig.11D**), probably due to the lack of inflammasome activation.

However, since THP-1 cells does not express p16, we tested the expression levels of other markers of senescence, such as CDK p21 and SIRT1. p21 protein levels were significantly increased whereas SIRT1 levels were decreased, in HgSMs compared to control cells (**fig.11E**).

Overall, our observations suggest that hyperglycemia induce a senescent phenotype in macrophages, but it seems not accompanied by a proper acquisition of classical SASP.

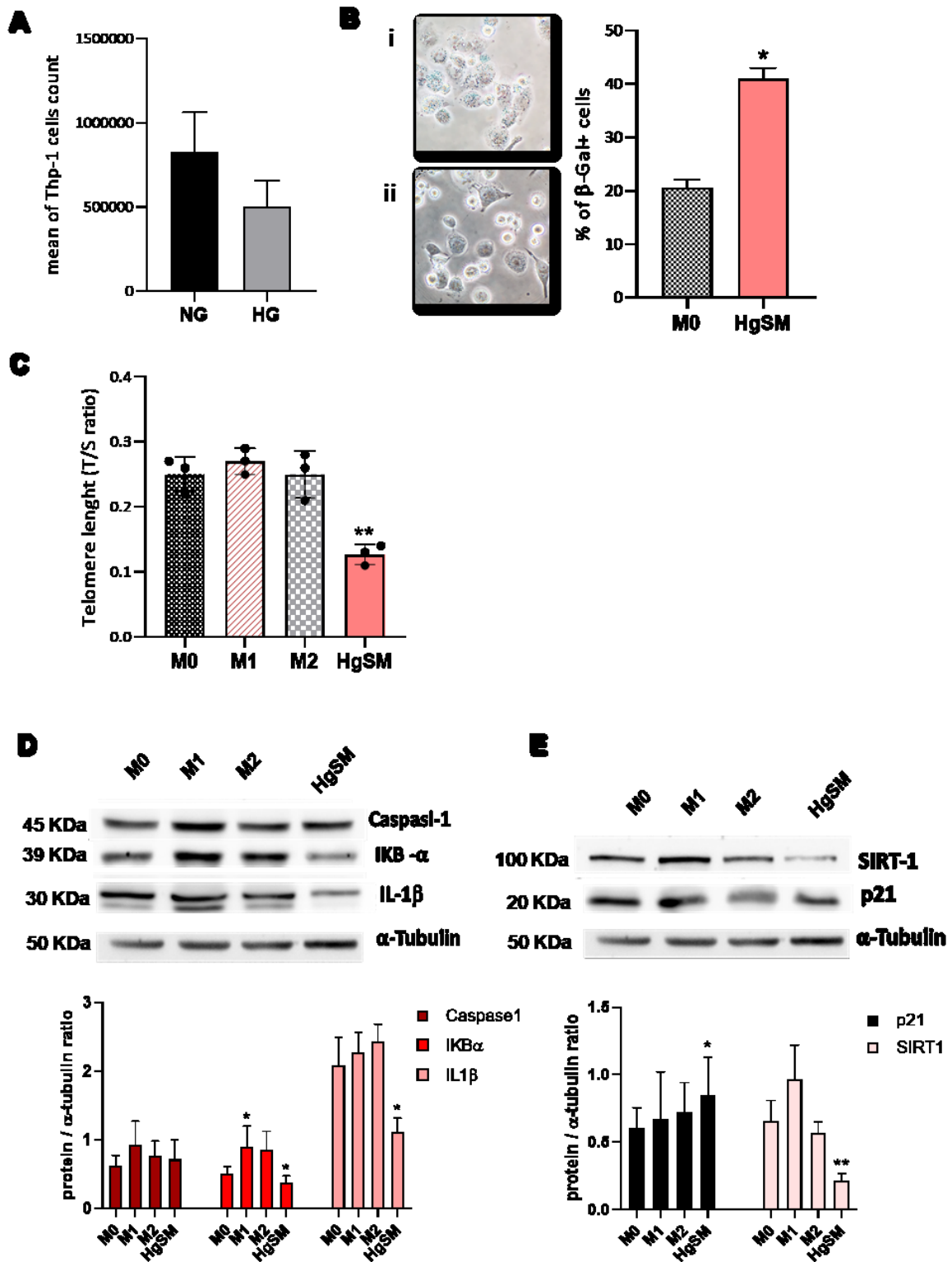


**Figure 11. Analysis of senescent features in HgSMs** A. Thp-1 proliferative activity in hyperglycemia compared to normoglycemia. B. SA- $\beta$ -Gal activity of HgSM(i) compared to M0(ii). C. measurements of telomere length (T/S ratio). D. western blot analysis of proteins involved in inflammation and E. senescence pathways. \* $p \leq 0.05$ ; \*\* $p \leq 0.01$

### 4.2.3 Human multipotent adipose tissue-derived stem (hMADS) cells differentiate into white adipocytes

In order to analyze the interactions between macrophages and adipocytes, we took advantage of the primary cells line hMADS that can be induced to differentiate into adipocytes.

By light microscopy, Oil Red O staining performed at various stages of adipose differentiation we observed the well-known morphological progression of hMADS cells from fibroblast-like cells devoid of lipids to roundish cells with a multilocular lipid content, typical of fully differentiated hMADS adipocytes (**fig. 12A**). Between days 12 and 15 of differentiation, about 80% of cells showed an abundant multilocular lipid content.

By RT-PCR, hMADS adipocytes (unlike their undifferentiated counterparts) expressed the typical markers of mature white adipocytes, including peroxisome proliferator-activated receptor  $\gamma$  (PPAR $\gamma$ ), fatty acid-binding protein 4 (FABP4), perilipin, and adiponectin (**fig. 12B**).

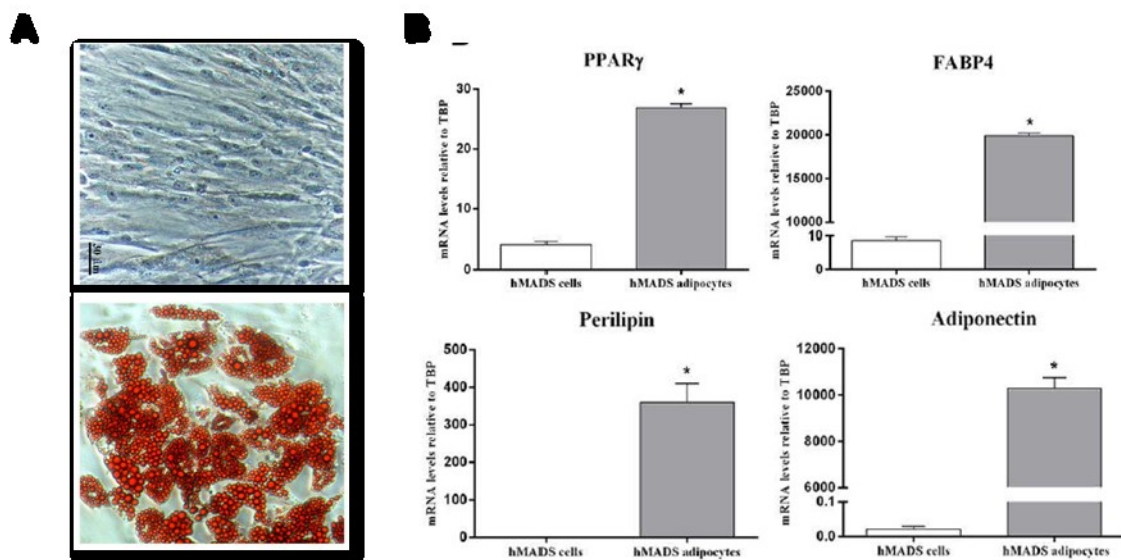


**Figure 12. hMADS cells differentiate into hMADS adipocytes.** A. Representative pictures from Oil Red O-stained confluent hMADS cells (day 0, left panel) and adipocytes (day 13, right panel). B. qRT-PCR analysis of PPAR $\gamma$ , FABP4, perilipin, and adiponectin expression in hMADS cells (white bars) and adipocytes (gray bars). \* $p < 0.05$

#### **4.2.4 HgSMs move towards a pro-inflammatory phenotype when cocultured with adipocytes**

The interactions between macrophages and adipocytes is a crucial mechanism to dissect the role of adipose tissue during obesity and obesity-related T2DM. We hypothesized that macrophages with senescence features could be involved in such complex interaction with adipocytes.

To verify our hypothesis, we set up a coculture of M0, M1, M2 and HgSM macrophages, and HMADs adipocytes. In coculture condition the two populations, macrophages and adipocytes, can interact through a porous (0.2µm pores) membrane for 48 hours (**fig.13A**).

Interestingly, real-time PCR analysis of HgSMs demonstrated a significant increased expression levels of the pro-inflammatory cytokines TNF- $\alpha$ , IL-6 and IL-8 and significant reduced levels of the anti-inflammatory IL-10 in comparison with M0 condition. Instead, M1 showed the typical high expression of IL-6 together with a low level of IL-10 (**fig.13B**). We also observed a significant decreasing expression of SIRT1 in the polarized macrophages M1, M2 and HgSM compared to M0 (**fig.13C**). Moreover, the coculture of HgSMs with HMADs adipocytes significantly increases the expression of miR-21 in HgSMs (**fig. 13D**). Finally, insulin (100 nM for 20 minutes) was added to the coculture medium. Interestingly, HgSM showed an increased amount of caspase 1 protein level, significantly higher respect to M0 macrophages. We also evaluated the activation of JNK by its phosphorylation that appeared increased in HgSM compared to control (**fig. 13D**).

In summary we can speculate that macrophages in the presence of adipocytes and insulin activate the JNK pathway which leads to release of the M1-like cytokines inducing insulin resistance and that hyperglycemia enhances this signaling.

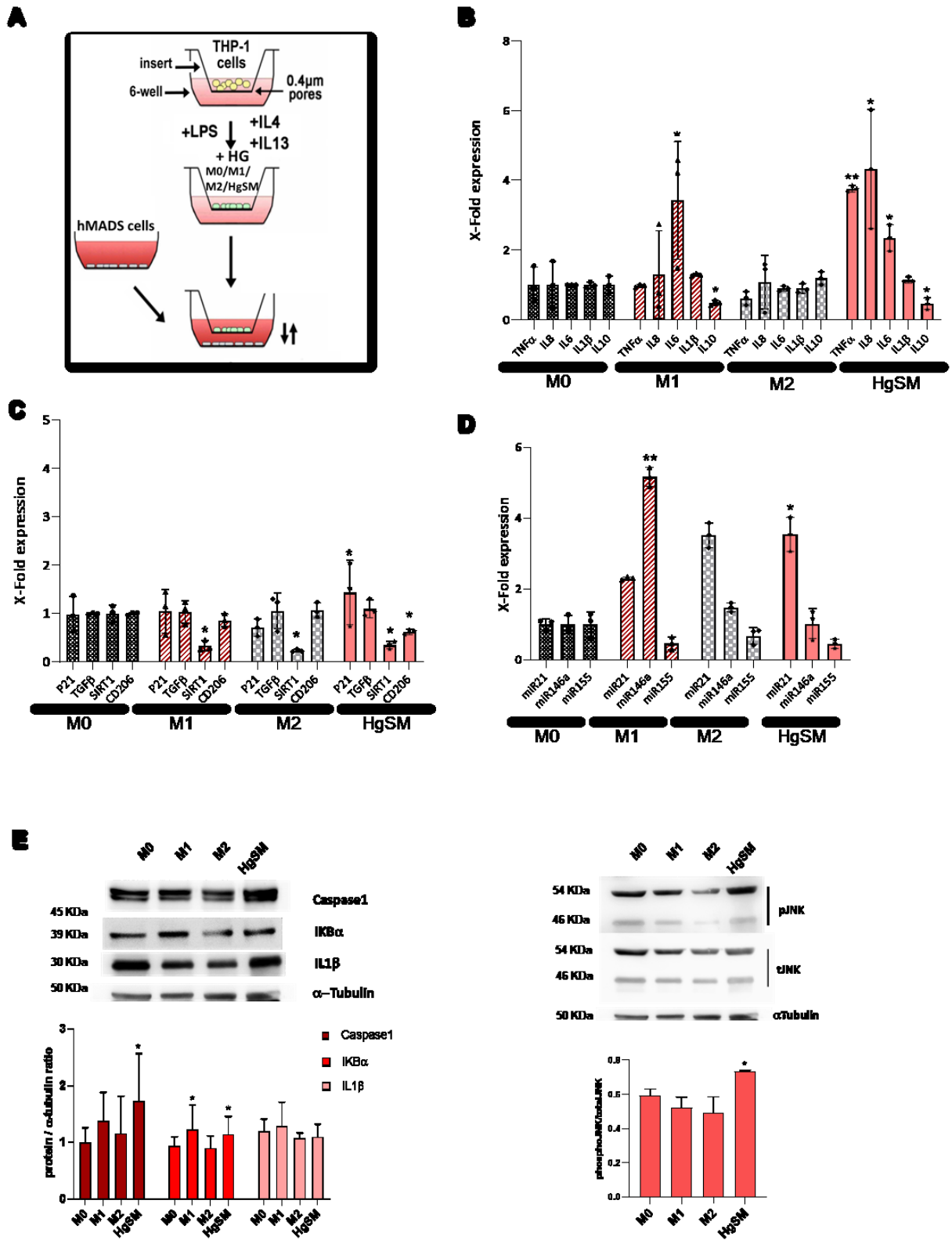


**Figure 13. The proinflammatory phenotype of HgSM when cocultured with HMADS adipocytes. A.** Diagram of the coculture experiment (THP1 on the insert above; HMADS on the well). **B.** mRNA expression analysis by RT-PCR. **C.** miRNA expression analysis by RT-PCR. **D and E.** western blot analysis. \* $p \leq 0.05$ ; \*\* $p \leq 0.01$



#### **4.2.5 Adipocytes exhibit a high inflammation burden when coculture with HgSMs, only at mRNA expression level**

Surprisingly, HMADs adipocytes cocultured with HgSM macrophages showed an important up-regulation of the pro-inflammatory cytokines TNF- $\alpha$ , IL-6, IL-8, IL-1- $\beta$ , compared to the HMADs adipocytes (CTR). In addition, even MCP-1 expression was found to increase in HMADs cocultured with HgSMs compared to control, whereas TGF- $\beta$  appeared significantly highly expressed in hMADs adipocytes cocultured with M1, M2 and HgSM compared to coculture with M0. Finally, adiponectin was significantly reduced only in HMADs adipocytes with M1 macrophages (**fig. 14A**).

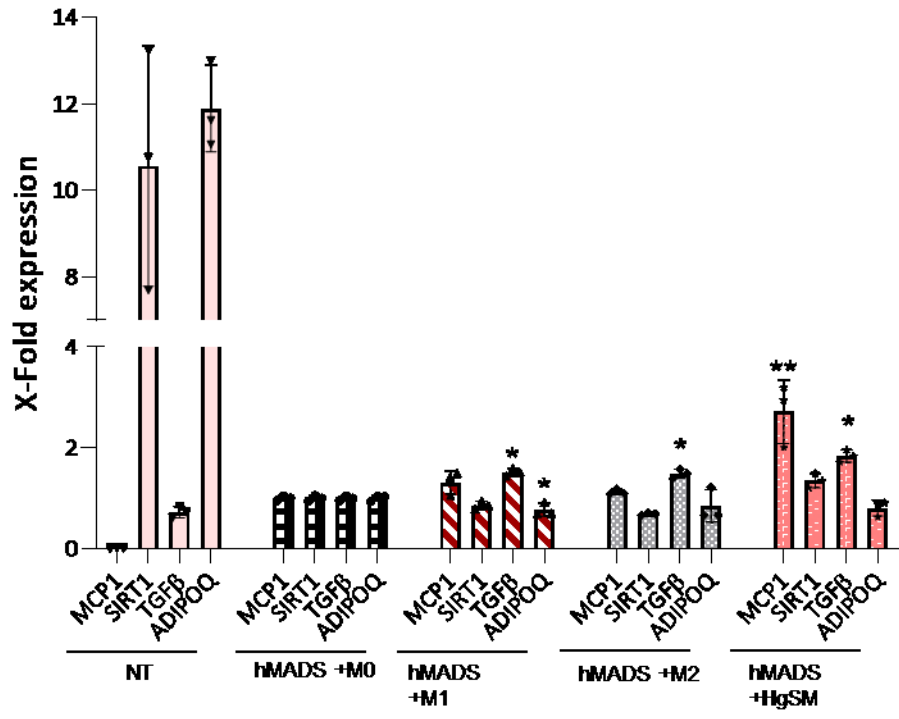
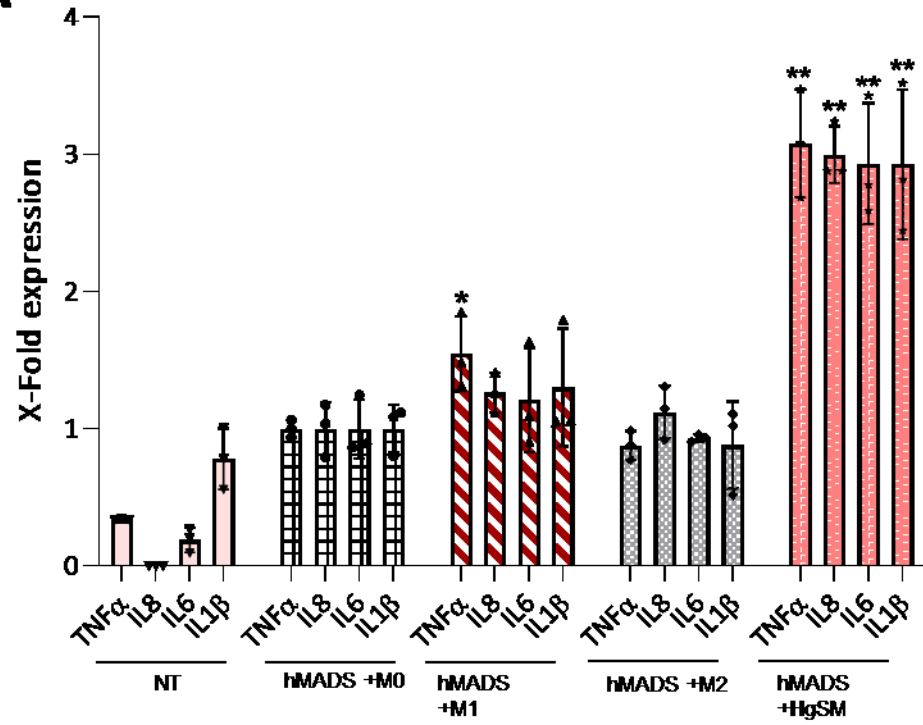
In HMADs adipocytes, we observed a significant activation of the inflammatory pathway when cocultured with macrophages, independently from their polarization compared to HMADs alone (NT).

Indeed, JNK phosphorylation in adipose cells was significantly increased with M0, M1, M2 and HgSM coculture as well as IKB $\alpha$  and SIRT1 that were found reduced in all the condition compared to NT (**fig.14B**).

Overall, even if we observed that hyperglycemia-treated macrophages fostered the inflammation in HMADs adipocytes at mRNA level, a significant correlation with protein levels was not observed.

Further analysis are mandatory in order to deciphering these results.

**A**



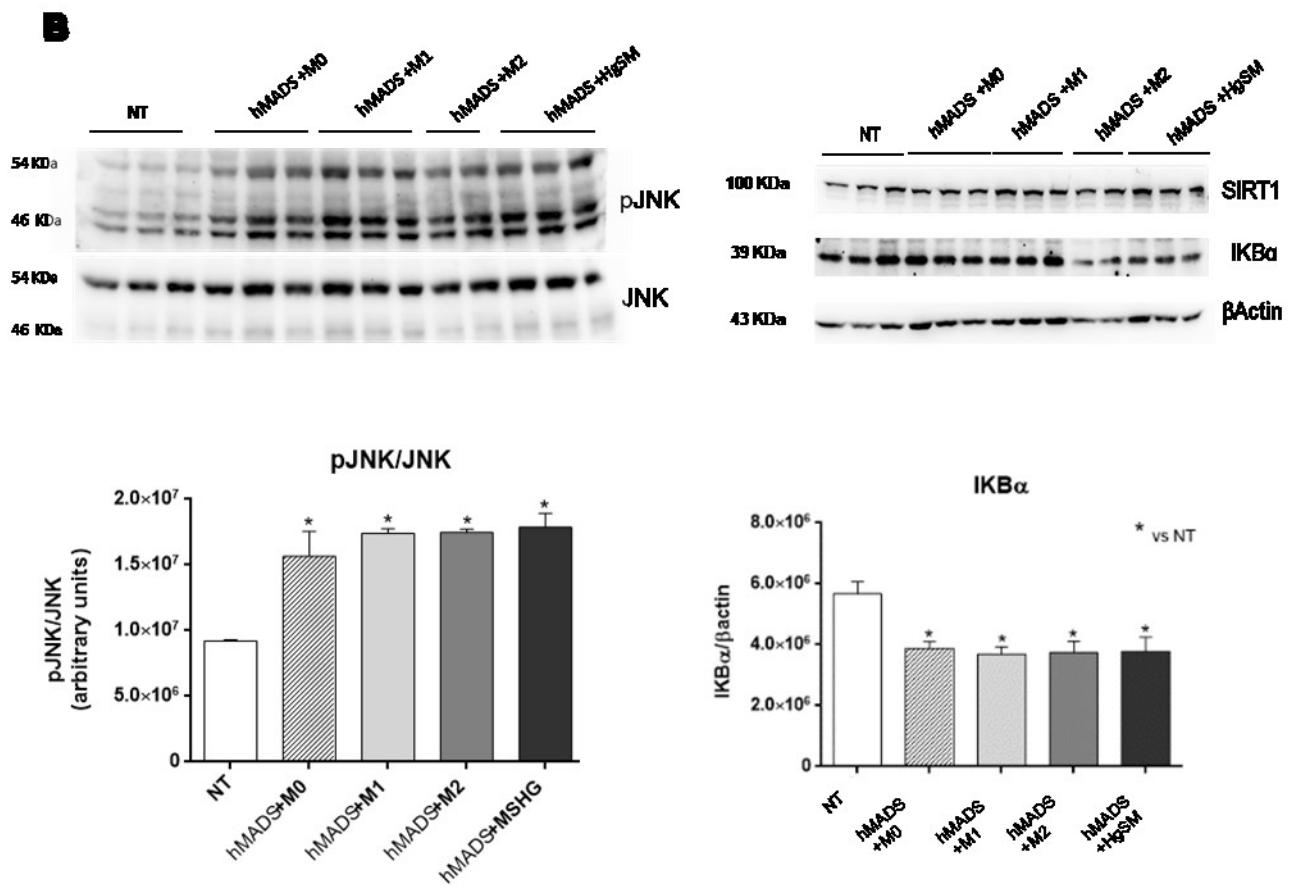


**Figure 14.** HMADS adipocytes exhibits a pro-inflammatory pattern at mRNA expression level. A. mRNA expression analysis by RT-PCR. B. Western blot analysis. \* $p < 0.05$ ; \*\* $p \leq 0.01$

### 4.3 Cytofluorimetric analysis

#### 4.3.1 Age-related M1/M2 phenotype changes in circulating monocytes from healthy individuals and AMI patients

In a previous published paper, we assessed the modulation of the monocyte subsets (classical, non-classical and intermediate) as well as the expression of CD80 and CD163 as markers of M1 and M2 phenotype respectively. within the subpopulation among age-matched healthy and unhealthy individuals. 21 elderly patients with acute myocardial infarction (AMI) and obesity-related morbidity were enrolled for this study, as well as 31 healthy control (CTR) individuals, grouped into a younger and an older age subjects (cut-off, 65 years).

The percentage of total (CD14+) monocytes was significantly greater in older than in younger CTR subjects (**fig. 15A**), whereas the differences between younger and older CTR subjects for monocyte subset were not significant (**fig. 15B**).

Calculation of the proportion of monocytes expressing the four CD80/CD163 biomarker combinations, such as CD80+, CD163+, CD80+CD163+ and CD80-CD163- in 31 healthy individuals demonstrated that the proportion of CD163+ cells among classical monocytes was significantly lower in older than in younger CTR subjects ( $2.1 \pm 2.2$  vs.  $4.2 \pm 2.8$ ;  $p=0.03$ ). The same was true for CD80-CD163- cells ( $1.1 \pm 1.2$  vs.  $2.7 \pm 2.4$ ;  $p=0.048$ ) (**fig. 15C**). The frequency of CD80-CD163- (**fig. 15C(i)**), Spearman's rho, 0.68;  $p<0.01$ ) and CD163+ (**fig. 15C(ii)**), Spearman's rho, 0.56;  $p<0.01$ ) classical monocytes correlated inversely with age.

Moreover, the proportion of CD163+ cells among non-classical monocytes was significantly higher in older than in younger CTR subjects ( $31.1 \pm 13.8$  vs.  $20.4 \pm 14.9$ ,  $p<0.05$ ) (**fig. 15D**).

Collectively, these data suggest that healthy aging is associated with: i) a reduction in CD163+ and CD80- CD163- classical monocytes and ii) an increase in CD163+ non-classical monocytes.

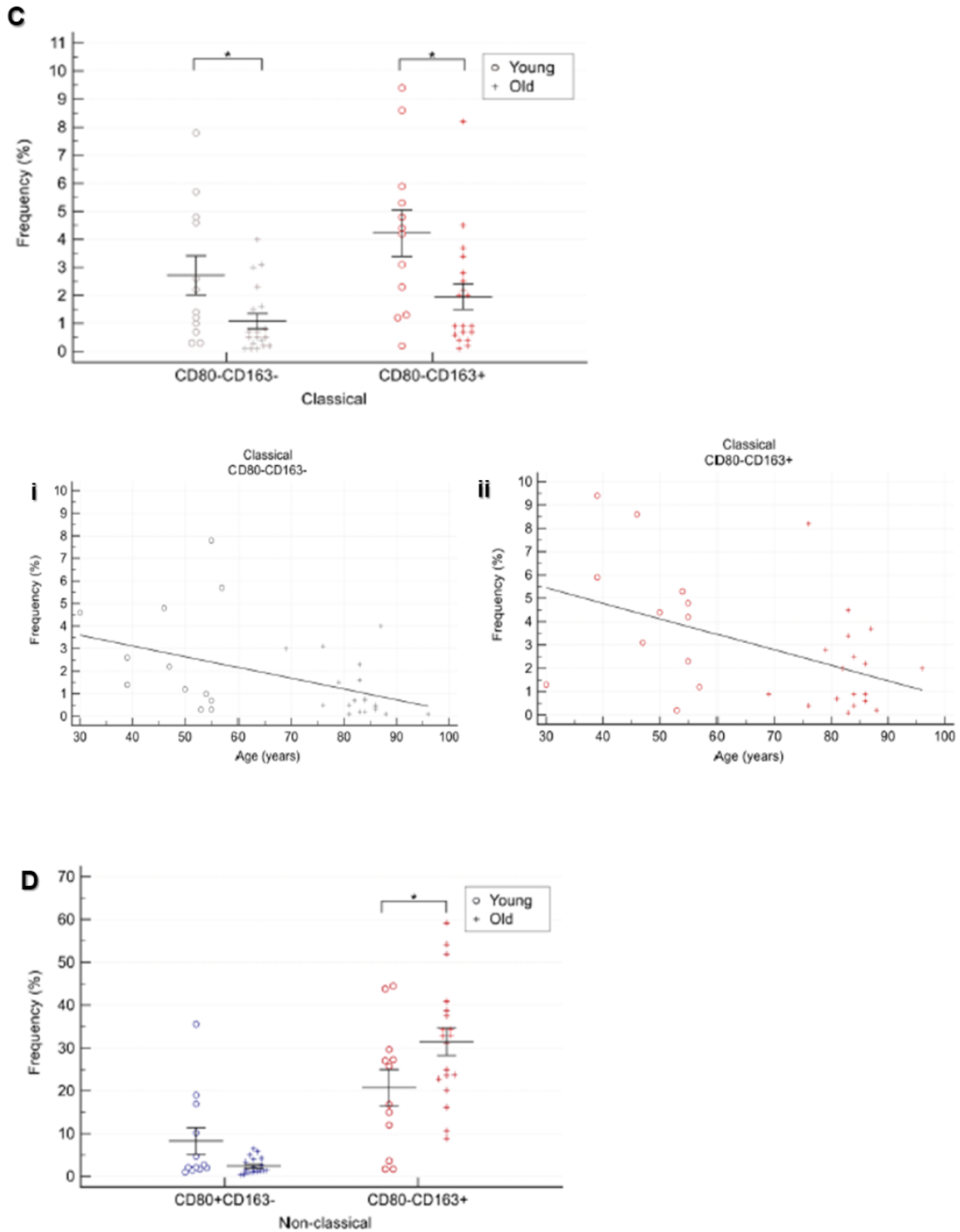


**Figure 15. Comparison of total monocyte (CD14+), monocytes subsets and CD80/CD163 cells proportion among monocyte subsets in older and younger CTR subjects. A. total monocyte (CD14+) and B. monocytes subsets (classical, intermediate and non-classical). C. proportion of CD80-CD163- and CD163+ cells among classical monocytes and age-related correlation of CD80-CD163- (i) and CD163+ (ii) classical monocytes. D. proportion of CD80+ and CD163+ among non-classical monocytes. \* $p < 0.05$ .**

Subsequently, comparison of CD80 and CD163 expression in classical, intermediate, and non-classical monocytes from AMI patients and older CTR individuals demonstrated a significantly lower proportion of CD80 and CD163 double-positive classical monocytes in AMI patients compared to older CTRs ( $70.1\pm 25.7$  vs.  $89\pm 5.6$ ,  $p<0.01$ ) and a significantly higher proportion of the CD80- CD163+ ( $6.7\pm 4.6$  vs.  $2.1\pm 2.2$ ,  $p<0.01$ ) and CD80-CD163- subsets ( $8.2\pm 12.1$  vs.  $1.1\pm 1.2$ ,  $p=0.02$ ) (**fig. 16A**).

As regards intermediate monocytes, double-negative cells were significantly more frequent in AMI patients ( $8.61\pm 9.91$  vs.  $3.81\pm 3.62$ ,  $p=0.049$ ), as well as CD80 single-positive cells ( $13.11\pm 12.96$  vs.  $5.52\pm 4.91$ ,  $p=0.02$ ) (**fig.16B**). Finally, AMI was associated with a greater frequency of non-classical CD80 single-positive cells ( $5.4\pm 5.5$  vs.  $2.4\pm 1.9$ ,  $p=0.02$ ) (**fig.16C**).

Altogether, these data highlight that AMI patients are characterized i) by extensive and complex changes in monocytes, particularly the classical and intermediate subsets; and ii) by substantial monocyte activation and differentiation, especially a decline of CD80 and CD163 double-positive (quiescent) classical monocytes and an increase in CD163+ cells, an opposite trend to that observed in healthy aging. Moreover, the proportion of CD80 single-positive (M1 phenotype) cells increased in intermediate and non-classical monocytes.

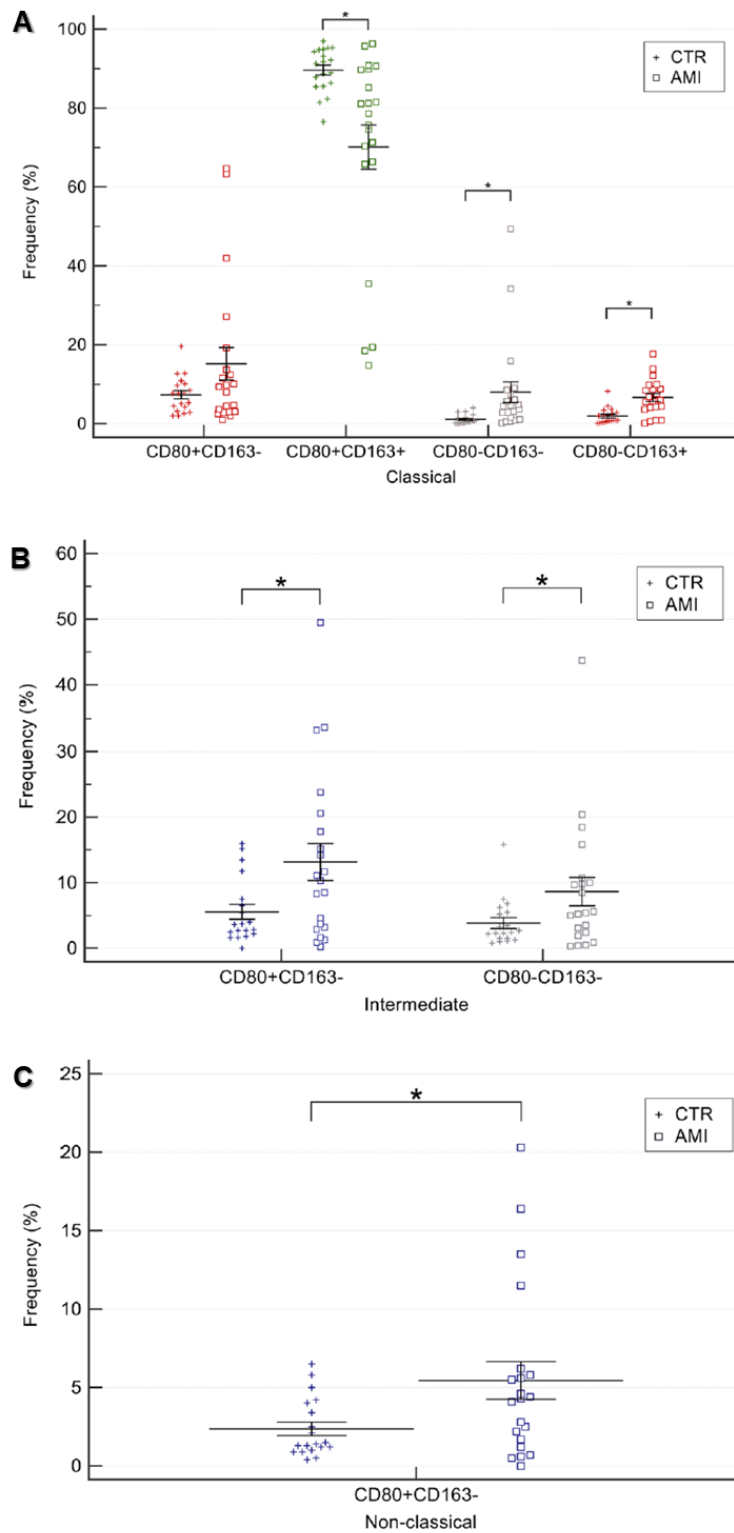


**Figure 16. Comparison of CD80/CD163 monocytes subsets among classical, intermediate and non-classical monocytes in AMI patients and older CTR subjects. A.** Classical, **B.** intermediate, **C.** non-classical monocytes. AMI = 21 patients affected by AMI, older than 65 years. Old = 19 healthy subjects older than 65 years. \* $p < 0.05$ .

#### **4.3.2 Evaluation of senescence in circulating monocyte subsets and their M1/M2 phenotype by flow cytometry**

Since senescent cells are known to accumulate with age, as we have already discussed, we investigated the percentage of senescent monocytes with cytofluorimetric analysis.

Then, as we demonstrated that M1/M2 phenotype within monocyte subpopulations was modulated in relation to age and in pathological condition, we were interested in understanding which subset mostly expressed the SA- $\beta$ -Gal activity.

To this aim, we analyzed blood samples from a small group of elderly individuals (75-85 years) by flow cytometry. Particularly, in this preliminary phase, we set up a cytofluorimetric analysis to detect SA- $\beta$ -Gal activity in monocyte subpopulations and M1/M2 polarization (**fig. 17A**).

Interestingly, we observed that non-classical subset had the most elevated SA- $\beta$ -Gal activity among the subpopulations and non-classical and intermediate monocytes showed a significant higher SA- $\beta$ -Gal activity (expressed as median of FITC intensity) compared to classical subpopulations in the total group of elderly subjects (**fig. 17B**).

Furthermore, we compared the senescence status of the M1(CD80+ CD163-) and the M2 (CD80- CD163+) phenotypes within the three subpopulations. We found that the M2 subgroups expressed a significant higher SA- $\beta$ -Gal activity compared to M1 subgroups in classical, intermediate and non-classical monocytes (**fig.17C**). In particular, the M2 polarization in non- classical and intermediate showed an increased activity of the SA-marker compared to the M2- polarization in classical monocytes (**fig.17D**).

To summarize, these preliminary data suggested that non-classical monocytes express the major senescent phenotype that is associated with the M2 phenotype. These results matched with recent published papers.



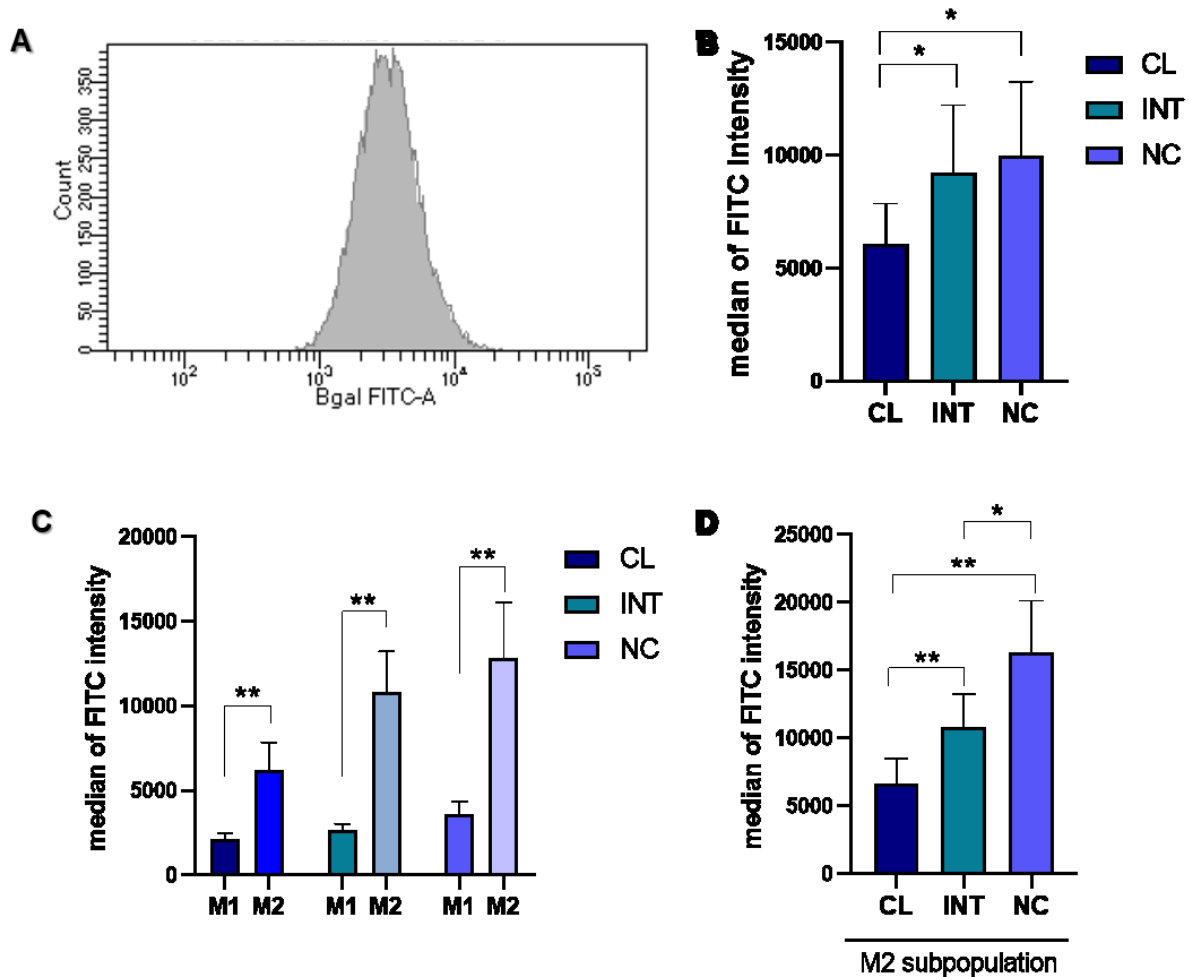


**Figure 17. Evaluation of SA- $\beta$ -Gal activity in M1/M2 monocyte subsets by flow cytometry.** **A.** histogram of FITC intensity per cells number within a population. **B.** comparison of SA- $\beta$ -Gal activity in classical, intermediate and non-classical monocytes. **C.** comparison of SA- $\beta$ -Gal activity in M1 (CD80+ CD163-) and M2 (CD80-CD163+) phenotype within each monocyte subsets **D.** comparison of SA- $\beta$ -Gal activity in M2 (CD80-CD163+) among the three subsets. \* $p=0.05$ ; \*\* $p\leq 0.01$ .

#### ***4.4 Circulating miR-146a shows age- and gender-specific trajectories in healthy aging and type 2 diabetes***

To evaluate the combined effect of age and glycemic state on circulating levels of the inflammatory miR-146a levels, 188 healthy subjects (CTR) aged 20-104 years and 144 type-2 diabetic patients (T2DM), aged 40-80 years, were analyzed. Our paper published in *Mechanism of Ageing and Development* (Mensa, Giuliani et al. 2019) demonstrated the following results:

- Circulating microRNA-146a levels show a significant age-related decline.
- MiR-146a shows gender-related correlations with specific biochemical variables.
- MiR-146a is overexpressed in type 2 diabetes patients treated with metformin.
- MiR-146a levels follow inverted U-shaped trajectories in healthy/unhealthy aging.

Thus, we have concluded that miR-146a could represent a functional biomarker of healthy/unhealthy aging.

#### ***4.5 Modulation of plasmatic $\beta$ -Galactosidase activity in healthy subjects is age-dependent***

Briefly, in this study published in *Oncotarget* (Spazzafumo, Mensa et al. 2017) we measured  $\beta$ -Gal activity by a fluorometric assay in plasma samples of 230 healthy subjects (55-87 years) and 230 T2DM patients. We observed a significant age-related increase of plasmatic  $\beta$ -Gal activity in healthy subjects whereas the enzymatic activity was significantly reduced in T2DM patients (n. 230; 55-96 years) compared to healthy subjects.

#### ***4.6 miR-222 and NF-light as new CSF biomarkers in age-related dementias***

In this study published in *Aging* (Marchegiani, Maticchione et al. 2019), we assess the diagnostic performance of cerebrospinal fluid (CSF) biomarkers across patients affected by either Alzheimer's disease (AD), tauopathies other than AD (TP), or vascular dementia (VD), and cognitively normal subjects (CNS). We recruited 153 patients and tested for classical AD CSF biomarkers- Amyloid- $\beta$ 42 and tau proteins - and novel candidate biomarkers - neurofilament (NF-) light and microRNA (miR) -21, -125b, -146a, and -222.

Of the four miRNAs analyzed, miR-222 levels were significantly increased in VD patients compared to both CNS and AD. Moreover, we found that all dementia patients had significantly higher concentrations of NF-light compared to CNS, with the TP group displaying the highest NF-light values, while male showed an increased level of NF-light when patients were grouped by gender. A significant inverse correlation was also observed between NF-light and cognitive impairment. In addition, NF-light showed a better diagnostic performance than miR-222 and classical AD biomarkers in differentiating TP and VD from CNS.

Overall, our results suggest that CSF NF-light and miR-222 are promising biomarkers that may help to diagnose non-AD disorders.

## 5. Discussion and Conclusion

Obesity is a powerful risk factor for many age-related diseases (ARDs), such as hypertension, dyslipidemia, cardiovascular complications, impaired glucose tolerance or Type 2 diabetes mellitus (T2DM). It is characterized by a subclinical, chronic and low-grade inflammation that recently was denominated *metaflammation*. The term indicates the metabolically triggered inflammation, as it is mainly fostered by nutrient and metabolic surplus (Hotamisligil 2017).

Evidence showed that during obesity, inflammation has a crucial role in the development of insulin resistance, particularly due to macrophages infiltration into visceral adipose tissue in obese states, that eventually leads to T2DM progression.

Senescent cells have also been found to accumulate in adipose tissue of obese and diabetic humans and mice (Minamino, Orimo et al. 2009, Villaret, Galitzky et al. 2010, Schafer, White et al. 2016) but it is unclear if their presence is a causal driver.

Adipose tissue is mainly distributed into two body compartments with different metabolic characteristics: subcutaneous adipose tissue (SAT) and visceral adipose tissue (VAT).

By histological analysis, we found a significant higher number of SA- $\beta$ -Gal positive cells in VAT compared to SAT of obese individuals. Moreover, we observed a significant elevated level of miR-146a as well as an increasing trend of the other two major *inflammamirs*, miR-21 and miR-155 in VAT compared to SAT. It is well-known that visceral adiposity is associated with several pathologies, including ARDs. Indeed, as hormonally active tissue, VAT releases hormones, cytokines and even microRNAs. Thus, based on previous literature we confirmed VAT as site of inflammation burden. Notably, we suggest that accumulation of senescent cells within adipose tissue might fuel the inflammatory status in obese individuals.

Then we observed that the majority of senescent cells in VAT and SAT were positive for the pan-macrophage marker CD68.

Even if macrophages expressing senescence markers were found to occur naturally within the adipose tissue of aged mice, few data are still available in humans. Thus, our result is effectively a worthwhile achievement. In addition, the number of SCs was found positively correlated with BMI in VAT but not in SAT samples.

The collected data suggest that the accumulation of senescent macrophages is strictly related to visceral adiposity expansion. Indeed, obesity induces the secretion of MCP-1, resulting in circulating monocytes recruitment into adipose tissue and their differentiation into macrophages, which eventually could become senescent.

Recently, we have published a study conducted in a mouse model of short-term sustained hyperglycemia to investigate senescence and inflammation in kidney, a prototypical organ damaged by diabetes. We have demonstrated a direct link between hyperglycemia and the senescent-associated secretory phenotype (SASP) in endothelial cells and macrophages, suggesting that SASP is a highly likely contributor to the fueling of low-grade inflammation.

Thus, in this thesis we evaluated the effect of hyperglycemia on macrophage polarization, by taking advantage of the commonly used THP1 cell line. THP1 cells were induced to differentiate by PMA stimulus and subsequently polarized in different phenotypes.

We showed that, after a week of treatment, hyperglycemia trigger a polarization toward a mixed M1/M2-like phenotype. Recently another paper has supported our findings (Moganti, Li et al. 2017). The hypothesis is actually that hyperglycemia trigger a condition similar to the immunoparalysis which occurs in septic shock. This condition is characterized by the simultaneous production of inflammatory and anti-inflammatory mediators, these latter to limiting the severity of the pro-inflammatory systemic effects. Furthermore, we showed hyperglycemia induced a senescent phenotype in macrophages, but it seems not accompanied by a proper SASP.

Hyperglycaemia is known to induce senescence in vitro. However, there is no evidence that high glucose is a direct cause of SASP acquisition. It is also unclear whether it can trigger a secretory profile comparable to the one induced by classic pro-senescence stimuli, e.g. replicative exhaustion.

Therefore, we decided to explore if the interaction of hyperglycemia-induced senescent macrophages (HgSMs) with adipocytes could affect their features and polarization.

To do this, we set up a coculture of M0, M1, M2 and HgSM macrophages with HMADs adipocytes, in which the two population could interact to each other through a porous (0.2µm pores) membrane for 48 hours. Conversely to the mixed phenotype of HgSMs, we observed a significant elevated expression of the pro-inflammatory and a diminished level of the anti-inflammatory cytokines in HgSM when cocultured with HMADs adipocytes.

Moreover, the presence of HMADs adipocytes significantly increases the expression of miR-21.

Then, when we added insulin to the coculture, HgSM showed the accumulation of caspase1 and activation of JNK by its phosphorylation, significantly higher respect to control macrophages.

It has been published that in a mouse model the JNK inactivation in myeloid cells led to reduce macrophage accumulation in adipose tissue and the expression of M1 cytokines. This indicate that JNK activity in adipose tissue macrophages is required for their activation during obesity (Han, Jung et al. 2013). Indeed, we found that, in turn, HMADs adipocytes showed an important up-regulation of several pro-inflammatory cytokines when cocultured with HgSM macrophages.

Overall, we proposed that macrophages in the presence of adipocytes and insulin activate the JNK pathway which leads to release of the M1-like cytokines inducing insulin resistance and that hyperglycemia enhances this signaling.

Studies on mice bone marrow transplantation have established that most macrophages found in the adipose tissue are derived from blood monocytes (Weisberg, McCann et al. 2003); a concept confirmed by in vivo monocyte labeling (Lumeng, Bodzin et al. 2007).

In a recent published paper, we evaluated the modulation of circulating monocyte subsets as well as the expression of M1/M2 markers in healthy elderly individuals compared to elderly patients with acute myocardial infarction (AMI), one of the major obesity-related morbidity.

By comparing young against aged individuals, we observed a reduction in CD163<sup>+</sup> and CD80-CD163<sup>-</sup> classical monocytes and an increase in CD163<sup>+</sup> non-classical monocytes in elderly.

On the contrary, AMI patients displayed an extensive and complex changes in monocytes, particularly the classical and intermediate subsets along with a substantial monocyte activation and differentiation, especially a decline of CD80 and CD163 double-positive classical monocytes and an increase in CD163<sup>+</sup> cells.

These findings agree with studies reporting that CD163<sup>+</sup> macrophages have a role in promoting atherosclerosis by enhancing inflammation and vascular permeability, and that they contribute to cardiac remodeling after AMI (Hulsmans, Sam et al. 2016, Guo, Akahori et al. 2018).

Moreover, it was found an association between monocyte surface CD163 and insulin resistance in patients with type 2 diabetes (Kawarabayashi, Motoyama et al. 2017).

Finally, we further investigated on the accumulation and distribution of circulating senescent monocytes. In this preliminary phase, we detect SA- $\beta$ -Gal activity in monocyte subpopulations and M1/M2-polarized subgroups in elderly individuals by flow cytometry. Our promising results suggested that non-classical subset had the higher SA- $\beta$ -Gal activity compared to classical and intermediate monocytes. Moreover, within the non-classical subset, the M2 phenotype showed the highest intensity of the senescence marker.

In the human immune system, accumulation of senescent T cells, B cells, and even hematopoietic stem cells with age has recently been reported. Indeed, the concept of a senescent subset of monocytes is rather novel. For instance, Ong and colleagues reported that the human non-classical monocyte subset shows a pro-inflammatory phenotype which is attributed to senescence (Ong, Hadadi et al. 2018). As we believe in this innovative field, we plan to improve the analysis by

recruiting a larger cohort of individuals with the aim to compare healthy subject with patients affected by obesity-driven T2DM.

Another aim of my thesis project was to identify innovative age-related biomarkers for evaluating senescence status in healthy aged subjects and in patients affected by age/related diseases, precisely T2DM and neurodegenerative disease.

Over the past decade, increasing interest was focused on the study of specific circulating miRNA signatures that can predict healthy aging and the onset of ARDs and their complications.

Several studies have investigated circulating levels of miR-146a in the context of ARDs, but there is currently no data regarding its modulation during human aging and no conclusive results in T2DM patients. Our published study showed a significant age-related decline in miR-146a plasma levels in healthy individuals, with a marked reduction in the group of subjects aged 75 years or older. Moreover, when healthy subjects and T2DM patients were compared, male patients displayed significantly lower miR-146a levels than age-matched controls, while the same difference was not significant in females. Notably, after proper normalization, diabetic patients treated with metformin showed higher circulating levels of miR-146a. In conclusion, our findings corroborate the idea that circulating biomarkers of ARDs, including miRNAs, may be useful to early detect deviations from a physiological aging trajectory (Mensa, Giuliani et al. 2019).

MicroRNAs have been proposed as promising biomarkers even for neurodegenerative diseases.

The economic costs and social burden associated to neurodegenerative disease have motivated efforts to identify innovative biomarkers for accurate and timely diagnosis and effective treatments.

Thus, in another published study we compare the diagnostic performance of classical and novel CSF biomarkers across patients affected by AD and NAD, such as TP and VD, and cognitively normal subjects (CNS).



AD diagnosis is currently based on clinical evaluation, neuropsychological testing, neuro-imaging techniques, and cerebrospinal fluid (CSF) classical biomarkers (Dubois, Feldman et al. 2007). However, the diagnostic relevance of these biomarkers in non-AD dementia and in differentiating between AD and non-AD is still under investigation.

Regarding miRNAs levels, our study showed a significant increase of CSF miR-222 levels in VD patients, suggesting a potential role in supporting the diagnosis of vascular dementia. Indeed, miR-222 was previously defined as an anti-angiogenic miR, upregulated in vascular walls with neointimal lesion formation (Ahmed, Bakhashab et al. 2018).

NF-light are proteins belonging to the neuronal cytoskeleton and their increased levels in CSF are indicative of neuronal damages, and thus they are proposed as new biomarker for differential diagnosis. Interestingly, we showed that the TP group was characterized by the highest NF-light values, which, in turn, showed a better diagnostic performance than classical AD biomarkers in distinguishing TP from CNS. Therefore, we proposed that CSF NF-light could be useful in supporting the diagnosis of non-AD dementia in combination with imaging and clinical data (Marchegiani, Maticchione et al. 2019).

## 6. References

- Ahima, R. S. (2009). "Connecting obesity, aging and diabetes." Nat Med **15**(9): 996-997.
- Ahmed, F. W., S. Bakhashab, I. T. Bastaman, R. E. Crossland, M. Glanville and J. U. Weaver (2018). "Anti-Angiogenic miR-222, miR-195, and miR-21a Plasma Levels in T1DM Are Improved by Metformin Therapy, Thus Elucidating Its Cardioprotective Effect: The MERIT Study." Int J Mol Sci **19**(10).
- Allsopp, R. C., E. Chang, M. Kashefi-Azham, E. I. Rogaev, M. A. Piatyszek, J. W. Shay and C. B. Harley (1995). "Telomere shortening is associated with cell division in vitro and in vivo." Exp Cell Res **220**(1): 194-200.
- Arner, P. and A. Kulyte (2015). "MicroRNA regulatory networks in human adipose tissue and obesity." Nat Rev Endocrinol **11**(5): 276-288.
- Ashwell, M., L. Mayhew, J. Richardson, B. Rickayzen. and (2014). "Waist-to-height ratio is more predictive of years of life lost than body mass index." PLoS One **9**: e103483.
- Baker, D. J., B. G. Childs, M. Durik, M. E. Wijers, C. J. Sieben, J. Zhong, R. A. Saltness, K. B. Jeganathan, G. C. Verzosa, A. Pezeshki, K. Khazaie, J. D. Miller and J. M. van Deursen (2016). "Naturally occurring p16(Ink4a)-positive cells shorten healthy lifespan." Nature **530**(7589): 184-189.
- Baker, D. J. and J. M. Sedivy (2013). "Probing the depths of cellular senescence." J Cell Biol **202**(1): 11-13.
- Biswas, S. K. and A. Mantovani (2010). "Macrophage plasticity and interaction with lymphocyte subsets: cancer as a paradigm." Nat Immunol **11**(10): 889-896.
- Boucher, J., A. Kleinriders and C. R. Kahn (2014). "Insulin receptor signaling in normal and insulin-resistant states." Cold Spring Harb Perspect Biol **6**(1).
- Bourlier, V., A. Zakaroff-Girard, A. Miranville, S. De Barros, M. Maumus, C. Sengenès, J. Galitzky, M. Lafontan, F. Karpe, K. N. Frayn and A. Bouloumie (2008). "Remodeling phenotype of human subcutaneous adipose tissue macrophages." Circulation **117**(6): 806-815.
- Braga, T. T., J. S. Agudelo and N. O. Camara (2015). "Macrophages During the Fibrotic Process: M2 as Friend and Foe." Front Immunol **6**: 602.
- Brakenhielm, E., R. Cao, B. Gao, B. Angelin, B. Cannon, P. Parini and Y. Cao (2004). "Angiogenesis inhibitor, TNP-470, prevents diet-induced and genetic obesity in mice." Circ Res **94**(12): 1579-1588.
- Brevig, K. and A. Esquela-Kerscher (2010). "The complexities of microRNA regulation: mirandering around the rules." Int J Biochem Cell Biol **42**(8): 1316-1329.
- Bu, L., M. Gao, S. Qu and D. Liu (2013). "Intraperitoneal injection of clodronate liposomes eliminates visceral adipose macrophages and blocks high-fat diet-induced weight gain and development of insulin resistance." AAPS J **15**(4): 1001-1011.
- Campisi, J. and F. d'Adda di Fagagna (2007). "Cellular senescence: when bad things happen to good cells." Nat Rev Mol Cell Biol **8**(9): 729-740.
- Cinti, S. (2005). "The adipose organ." Prostaglandins Leukot Essent Fatty Acids **73**(1): 9-15.

- Cinti, S. (2011). "Between brown and white: novel aspects of adipocyte differentiation." Ann Med **43**(2): 104-115.
- Cinti, S. (2012). "The adipose organ at a glance." Dis Model Mech **5**(5): 588-594.
- Cinti, S., M. C. Zingaretti, R. Canello, E. Ceresi and P. Ferrara (2001). "Morphologic techniques for the study of brown adipose tissue and white adipose tissue." Methods Mol Biol **155**: 21-51.
- Coppe, J. P., P. Y. Desprez, A. Krtolica and J. Campisi (2010). "The senescence-associated secretory phenotype: the dark side of tumor suppression." Annu Rev Pathol **5**: 99-118.
- Coppe, J. P., C. K. Patil, F. Rodier, Y. Sun, D. P. Munoz, J. Goldstein, P. S. Nelson, P. Y. Desprez and J. Campisi (2008). "Senescence-associated secretory phenotypes reveal cell-nonautonomous functions of oncogenic RAS and the p53 tumor suppressor." PLoS Biol **6**(12): 2853-2868.
- Costantini, A., N. Viola, A. Berretta, R. Galeazzi, G. Maccachione, J. Sabbatinelli, G. Storci, S. De Matteis, L. Butini, M. R. Rippo, A. D. Procopio, D. Caraceni, R. Antonicelli, F. Olivieri and M. Bonafe (2018). "Age-related M1/M2 phenotype changes in circulating monocytes from healthy/unhealthy individuals." Aging (Albany NY) **10**(6): 1268-1280.
- Cowey, S. and R. W. Hardy (2006). "The metabolic syndrome: A high-risk state for cancer?" Am J Pathol **169**(5): 1505-1522.
- Czech, M. P. (2017). "Insulin action and resistance in obesity and type 2 diabetes." Nat Med **23**(7): 804-814.
- Dalmas, E., K. Clement and M. Guerre-Millo (2011). "Defining macrophage phenotype and function in adipose tissue." Trends Immunol **32**(7): 307-314.
- Debacq-Chainiaux, F., J. D. Erusalimsky, J. Campisi and O. Toussaint (2009). "Protocols to detect senescence-associated beta-galactosidase (SA-beta-gal) activity, a biomarker of senescent cells in culture and in vivo." Nat Protoc **4**(12): 1798-1806.
- Demaria, M., N. Ohtani, S. A. Youssef, F. Rodier, W. Toussaint, J. R. Mitchell, R. M. Laberge, J. Vijg, H. Van Steeg, M. E. Dolle, J. H. Hoeijmakers, A. de Bruin, E. Hara and J. Campisi (2014). "An essential role for senescent cells in optimal wound healing through secretion of PDGF-AA." Dev Cell **31**(6): 722-733.
- Devevre, E. F., M. Renovato-Martins, K. Clement, C. Sautes-Fridman, I. Cremer and C. Poitou (2015). "Profiling of the three circulating monocyte subpopulations in human obesity." J Immunol **194**(8): 3917-3923.
- Donath, M. Y. (2014). "Targeting inflammation in the treatment of type 2 diabetes: time to start." Nat Rev Drug Discov **13**(6): 465-476.
- Dou, Z., K. Ghosh, M. G. Vizioli, J. Zhu, P. Sen, K. J. Wangenstein, J. Simithy, Y. Lan, Y. Lin, Z. Zhou, B. C. Capell, C. Xu, M. Xu, J. E. Kieckhafer, T. Jiang, M. Shoshkes-Carmel, K. Tanim, G. N. Barber, J. T. Seykora, S. E. Millar, K. H. Kaestner, B. A. Garcia, P. D. Adams and S. L. Berger (2017). "Cytoplasmic chromatin triggers inflammation in senescence and cancer." Nature **550**(7676): 402-406.
- Dubois, B., H. H. Feldman, C. Jacova, S. T. Dekosky, P. Barberger-Gateau, J. Cummings, A. Delacourte, D. Galasko, S. Gauthier, G. Jicha, K. Meguro, J. O'Brien, F. Pasquier, P. Robert, M. Rossor, S. Salloway, Y. Stern, P. J. Visser and P. Scheltens (2007). "Research criteria for the diagnosis of Alzheimer's disease: revising the NINCDS-ADRDA criteria." Lancet Neurol **6**(8): 734-746.

- Engin, A. (2017). "The Definition and Prevalence of Obesity and Metabolic Syndrome." Adv Exp Med Biol **960**: 1-17.
- Farr, J. N., M. Xu, M. M. Weivoda, D. G. Monroe, D. G. Fraser, J. L. Onken, B. A. Negley, J. G. Sfeir, M. B. Ogrodnik, C. M. Hachfeld, N. K. LeBrasseur, M. T. Drake, R. J. Pignolo, T. Pirtskhalava, T. Tchkonina, M. J. Oursler, J. L. Kirkland and S. Khosla (2017). "Targeting cellular senescence prevents age-related bone loss in mice." Nat Med **23**(9): 1072-1079.
- Franceschi, C. (2017). "Healthy ageing in 2016: Obesity in geroscience - is cellular senescence the culprit?" Nat Rev Endocrinol **13**(2): 76-78.
- Franceschi, C., M. Bonafe, S. Valensin, F. Olivieri, M. De Luca, E. Ottaviani and G. De Benedictis (2000). "Inflamm-aging. An evolutionary perspective on immunosenescence." Ann N Y Acad Sci **908**: 244-254.
- Franceschi, C. and J. Campisi (2014). "Chronic inflammation (inflammaging) and its potential contribution to age-associated diseases." J Gerontol A Biol Sci Med Sci **69 Suppl 1**: S4-9.
- Gallagher-Beckley, A. J., L. Q. Lan, S. Aono, L. Wang and J. Shi (2013). "Caspase-1 activation and mature interleukin-1beta release are uncoupled events in monocytes." World J Biol Chem **4**(2): 30-34.
- Garraud, T., M. Harel, M. A. Boutet, B. Le Goff and F. Blanchard (2018). "The enigmatic role of IL-38 in inflammatory diseases." Cytokine Growth Factor Rev **39**: 26-35.
- Gioia, U., S. Francia, M. Cabrini, S. Brambillasca, F. Michelini, C. W. Jones-Weinert and F. d'Adda di Fagagna (2019). "Pharmacological boost of DNA damage response and repair by enhanced biogenesis of DNA damage response RNAs." Sci Rep **9**(1): 6460.
- Goossens, G. H. (2017). "The Metabolic Phenotype in Obesity: Fat Mass, Body Fat Distribution, and Adipose Tissue Function." Obes Facts **10**(3): 207-215.
- Gordon, E. J., S. Rao, J. W. Pollard, S. L. Nutt, R. A. Lang and N. L. Harvey (2010). "Macrophages define dermal lymphatic vessel calibre during development by regulating lymphatic endothelial cell proliferation." Development **137**(22): 3899-3910.
- Gorska, E., K. Popko, M. Winiarska and M. Wasik (2009). "[Pleiotropic effects of leptin]." Pediatr Endocrinol Diabetes Metab **15**(1): 45-50.
- Guo, L., H. Akahori, E. Harari, S. L. Smith, R. Polavarapu, V. Karmali, F. Otsuka, R. L. Gannon, R. E. Braumann, M. H. Dickinson, A. Gupta, A. L. Jenkins, M. J. Lipinski, J. Kim, P. Chhour, P. S. de Vries, H. Jinnouchi, R. Kutys, H. Mori, M. D. Kutyna, S. Torii, A. Sakamoto, C. U. Choi, Q. Cheng, M. L. Grove, M. A. Sawan, Y. Zhang, Y. Cao, F. D. Kolodgie, D. P. Cormode, D. E. Arking, E. Boerwinkle, A. C. Morrison, J. Erdmann, N. Sotoodehnia, R. Virmani and A. V. Finn (2018). "CD163+ macrophages promote angiogenesis and vascular permeability accompanied by inflammation in atherosclerosis." J Clin Invest **128**(3): 1106-1124.
- Hall, B. M., V. Balan, A. S. Gleiberman, E. Strom, P. Krasnov, L. P. Virtuoso, E. Rydkina, S. Vujcic, K. Balan, Gitlin, II, K. I. Leonova, C. R. Consiglio, S. O. Gollnick, O. B. Chernova and A. V. Gudkov (2017). "p16(Ink4a) and senescence-associated beta-galactosidase can be induced in macrophages as part of a reversible response to physiological stimuli." Aging (Albany NY) **9**(8): 1867-1884.
- Hall, B. M., V. Balan, A. S. Gleiberman, E. Strom, P. Krasnov, L. P. Virtuoso, E. Rydkina, S. Vujcic, K. Balan, I. Gitlin, K. Leonova, A. Polinsky, O. B. Chernova and A. V. Gudkov (2016). "Aging of mice is associated with p16(Ink4a)- and beta-galactosidase-positive macrophage accumulation that can be induced in young mice by senescent cells." Aging (Albany NY) **8**(7): 1294-1315.

- Han, M. S., D. Y. Jung, C. Morel, S. A. Lakhani, J. K. Kim, R. A. Flavell and R. J. Davis (2013). "JNK expression by macrophages promotes obesity-induced insulin resistance and inflammation." Science **339**(6116): 218-222.
- Hayflick, L. and P. S. Moorhead (1961). "The serial cultivation of human diploid cell strains." Exp Cell Res **25**: 585-621.
- Herbig, U., M. Ferreira, L. Condel, D. Carey and J. M. Sedivy (2006). "Cellular senescence in aging primates." Science **311**(5765): 1257.
- Hernandez-Segura, A., J. Nehme and M. Demaria (2018). "Hallmarks of Cellular Senescence." Trends Cell Biol **28**(6): 436-453.
- Hotamisligil, G. S. (2017). "Inflammation, metaflammation and immunometabolic disorders." Nature **542**(7640): 177-185.
- Hulsmans, M., F. Sam and M. Nahrendorf (2016). "Monocyte and macrophage contributions to cardiac remodeling." J Mol Cell Cardiol **93**: 149-155.
- Iyengar, N. M., C. A. Hudis and A. J. Dannenberg (2015). "Obesity and cancer: local and systemic mechanisms." Annu Rev Med **66**: 297-309.
- Kadowaki, T., T. Yamauchi, N. Kubota, K. Hara, K. Ueki and K. Tobe (2006). "Adiponectin and adiponectin receptors in insulin resistance, diabetes, and the metabolic syndrome." J Clin Invest **116**(7): 1784-1792.
- Kahn, S. E., R.L. Prigeon, R.S. Schwartz, W.Y. Fujimoto, R.H. Knopp, J.D. Brunzell and D. Porte. (2001). "Obesity, body fat distribution, insulin sensitivity and Islet beta-cell function as explanations for metabolic diversity." The Journal of Nutrition **131**: 354S–360S.
- Kang, K. S. (2011). "The secret lives of stem cells: unraveling the molecular basis of stem cell aging." Cell Cycle **10**(24): 4188.
- Kawarabayashi, R., K. Motoyama, M. Nakamura, Y. Yamazaki, T. Morioka, K. Mori, S. Fukumoto, Y. Imanishi, A. Shioi, T. Shoji, M. Emoto and M. Inaba (2017). "The Association between Monocyte Surface CD163 and Insulin Resistance in Patients with Type 2 Diabetes." J Diabetes Res **2017**: 6549242.
- Kirkland, J. L., T. Tchkonina, Y. Zhu, L. J. Niedernhofer and P. D. Robbins (2017). "The Clinical Potential of Senolytic Drugs." J Am Geriatr Soc **65**(10): 2297-2301.
- Kitada, K., D. Nakano, H. Ohsaki, H. Hitomi, T. Minamino, J. Yatabe, R. A. Felder, H. Mori, T. Masaki, H. Kobori and A. Nishiyama (2014). "Hyperglycemia causes cellular senescence via a SGLT2- and p21-dependent pathway in proximal tubules in the early stage of diabetic nephropathy." J Diabetes Complications **28**(5): 604-611.
- Komohara, Y., Y. Fujiwara, K. Ohnishi, D. Shiraishi and M. Takeya (2016). "Contribution of Macrophage Polarization to Metabolic Diseases." J Atheroscler Thromb **23**(1): 10-17.
- Kratz, M., T. Baars and S. Guyenet (2013). "The relationship between high-fat dairy consumption and obesity, cardiovascular, and metabolic disease." Eur J Nutr **52**(1): 1-24.

- Krishnan, J., C. Danzer, T. Simka, J. Ukropec, K. M. Walter, S. Kumpf, P. Mirtschink, B. Ukropcova, D. Gasperikova, T. Pedrazzini and W. Krek (2012). "Dietary obesity-associated Hif1alpha activation in adipocytes restricts fatty acid oxidation and energy expenditure via suppression of the Sirt2-NAD<sup>+</sup> system." Genes Dev **26**(3): 259-270.
- Kuilman, T., C. Michaloglou, W. J. Mooi and D. S. Peeper (2010). "The essence of senescence." Genes Dev **24**(22): 2463-2479.
- Kusminski, C. M., P. E. Bickel and P. E. Scherer (2016). "Targeting adipose tissue in the treatment of obesity-associated diabetes." Nat Rev Drug Discov **15**(9): 639-660.
- Lackey, D. E., R. G. Lazaro, P. Li, A. Johnson, A. Hernandez-Carretero, N. Weber, I. Vorobyova, H. Tsukamoto and O. Osborn (2016). "The role of dietary fat in obesity-induced insulin resistance." Am J Physiol Endocrinol Metab **311**(6): E989-E997.
- Lawless, C., C. Wang, D. Jurk, A. Merz, T. Zglinicki and J. F. Passos (2010). "Quantitative assessment of markers for cell senescence." Exp Gerontol **45**(10): 772-778.
- Lee, B. Y., J. A. Han, J. S. Im, A. Morrone, K. Johung, E. C. Goodwin, W. J. Kleijer, D. DiMaio and E. S. Hwang (2006). "Senescence-associated beta-galactosidase is lysosomal beta-galactosidase." Aging Cell **5**(2): 187-195.
- Ley, K. (2017). "M1 Means Kill; M2 Means Heal." J Immunol **199**(7): 2191-2193.
- Ley, R. E., F. Backhed, P. Turnbaugh, C. A. Lozupone, R. D. Knight and J. I. Gordon (2005). "Obesity alters gut microbial ecology." Proc Natl Acad Sci U S A **102**(31): 11070-11075.
- Lopez-Otin, C., M. A. Blasco, L. Partridge, M. Serrano and G. Kroemer (2013). "The hallmarks of aging." Cell **153**(6): 1194-1217.
- Lumeng, C. N., J. L. Bodzin and A. R. Saltiel (2007). "Obesity induces a phenotypic switch in adipose tissue macrophage polarization." J Clin Invest **117**(1): 175-184.
- Lumeng, C. N., S. M. Deyoung, J. L. Bodzin and A. R. Saltiel (2007). "Increased inflammatory properties of adipose tissue macrophages recruited during diet-induced obesity." Diabetes **56**(1): 16-23.
- Malaquin, N., A. Martinez and F. Rodier (2016). "Keeping the senescence secretome under control: Molecular reins on the senescence-associated secretory phenotype." Exp Gerontol **82**: 39-49.
- Mantovani, A., A. Sica, S. Sozzani, P. Allavena, A. Vecchi and M. Locati (2004). "The chemokine system in diverse forms of macrophage activation and polarization." Trends Immunol **25**(12): 677-686.
- Mantovani, A., S. Sozzani, M. Locati, P. Allavena and A. Sica (2002). "Macrophage polarization: tumor-associated macrophages as a paradigm for polarized M2 mononuclear phagocytes." Trends Immunol **23**(11): 549-555.
- Marchegiani, F., G. Maticchione, D. Ramini, F. Marcheselli, R. Recchioni, T. Casoli, E. Mercuri, M. Lazzarini, B. Giorgetti, V. Cameriere, S. Paolini, L. Paciaroni, T. Rossi, R. Galeazzi, R. Lisa, A. R. Bonfigli, A. D. Procopio, M. De Luca, G. Pelliccioni and F. Olivieri (2019). "Diagnostic performance of new and classic CSF biomarkers in age-related dementias." Aging (Albany NY) **11**(8): 2420-2429.
- Martinez, F. O. and S. Gordon (2014). "The M1 and M2 paradigm of macrophage activation: time for reassessment." F1000Prime Rep **6**: 13.

- McHugh, D. and J. Gil (2018). "Senescence and aging: Causes, consequences, and therapeutic avenues." J Cell Biol **217**(1): 65-77.
- Mensa, E., A. Giuliani, G. Maticchione, F. Gurau, A. R. Bonfigli, F. Romagnoli, M. De Luca, J. Sabbatinelli and F. Olivieri (2019). "Circulating miR-146a in healthy aging and type 2 diabetes: Age- and gender-specific trajectories." Mech Ageing Dev **180**: 1-10.
- Minamino, T. (2009). "[Role of the renin-angiotensin system in the regulation of vascular senescence]." Nihon Rinsho **67**(4): 715-722.
- Minamino, T., M. Orimo, I. Shimizu, T. Kunieda, M. Yokoyama, T. Ito, A. Nojima, A. Nabetani, Y. Oike, H. Matsubara, F. Ishikawa and I. Komuro (2009). "A crucial role for adipose tissue p53 in the regulation of insulin resistance." Nat Med **15**(9): 1082-1087.
- Miyazawa-Hoshimoto, S., K. Takahashi, H. Bujo, N. Hashimoto and Y. Saito (2003). "Elevated serum vascular endothelial growth factor is associated with visceral fat accumulation in human obese subjects." Diabetologia **46**(11): 1483-1488.
- Moganti, K., F. Li, C. Schmuttermaier, S. Riemann, H. Kluter, A. Gratchev, M. C. Harmsen and J. Kzhyshkowska (2017). "Hyperglycemia induces mixed M1/M2 cytokine profile in primary human monocyte-derived macrophages." Immunobiology **222**(10): 952-959.
- Moore, K. J. and I. Tabas (2011). "Macrophages in the pathogenesis of atherosclerosis." Cell **145**(3): 341-355.
- Morris, S. M., Jr. (2010). "Arginine: master and commander in innate immune responses." Sci Signal **3**(135): pe27.
- Munoz-Espin, D. and M. Serrano (2014). "Cellular senescence: from physiology to pathology." Nat Rev Mol Cell Biol **15**(7): 482-496.
- Murray, P. J. (2017). "Macrophage Polarization." Annu Rev Physiol **79**: 541-566.
- Musi, N., J. M. Valentine, K. R. Sickora, E. Baeuerle, C. S. Thompson, Q. Shen and M. E. Orr (2018). "Tau protein aggregation is associated with cellular senescence in the brain." Aging Cell **17**(6): e12840.
- Noy, R. and J. W. Pollard (2014). "Tumor-associated macrophages: from mechanisms to therapy." Immunity **41**(1): 49-61.
- Olivieri, F., M. R. Rippo, A. D. Procopio and F. Fazioli (2013). "Circulating inflamma-miRs in aging and age-related diseases." Front Genet **4**: 121.
- Ong, S. M., E. Hadadi, T. M. Dang, W. H. Yeap, C. T. Tan, T. P. Ng, A. Larbi and S. C. Wong (2018). "The pro-inflammatory phenotype of the human non-classical monocyte subset is attributed to senescence." Cell Death Dis **9**(3): 266.
- Palmer, A. K., B. Gustafson, J. L. Kirkland and U. Smith (2019). "Cellular senescence: at the nexus between ageing and diabetes." Diabetologia **62**(10): 1835-1841.
- Passos, J. F., G. Nelson, C. Wang, T. Richter, C. Simillion, C. J. Proctor, S. Miwa, S. Olijslagers, J. Hallinan, A. Wipat, G. Saretzki, K. L. Rudolph, T. B. Kirkwood and T. von Zglinicki (2010). "Feedback between p21 and reactive oxygen production is necessary for cell senescence." Mol Syst Biol **6**: 347.

- Perreault, M. and A. Marette (2001). "Targeted disruption of inducible nitric oxide synthase protects against obesity-linked insulin resistance in muscle." Nat Med **7**(10): 1138-1143.
- Piatkiewicz, P. and A. Czech (2011). "Glucose metabolism disorders and the risk of cancer." Arch Immunol Ther Exp (Warsz) **59**(3): 215-230.
- Prattichizzo, F., V. De Nigris, E. Mancuso, R. Spiga, A. Giuliani, G. Maccacchione, R. Lazzarini, F. Marcheselli, R. Recchioni, R. Testa, L. La Sala, M. R. Rippo, A. D. Procopio, F. Olivieri and A. Ceriello (2018). "Short-term sustained hyperglycaemia fosters an archetypal senescence-associated secretory phenotype in endothelial cells and macrophages." Redox Biol **15**: 170-181.
- Quinn, S. R. and L. A. O'Neill (2011). "A trio of microRNAs that control Toll-like receptor signalling." Int Immunol **23**(7): 421-425.
- Rhee, D. B., A. Ghosh, J. Lu, V. A. Bohr and Y. Liu (2011). "Factors that influence telomeric oxidative base damage and repair by DNA glycosylase OGG1." DNA Repair (Amst) **10**(1): 34-44.
- Ricard-Blum, S. (2011). "The collagen family." Cold Spring Harb Perspect Biol **3**(1): a004978.
- Ritschka, B., M. Storer, A. Mas, F. Heinzmann, M. C. Ortells, J. P. Morton, O. J. Sansom, L. Zender and W. M. Keyes (2017). "The senescence-associated secretory phenotype induces cellular plasticity and tissue regeneration." Genes Dev **31**(2): 172-183.
- Roos, C. M., B. Zhang, A. K. Palmer, M. B. Ogronnik, T. Pirtskhalava, N. M. Thalji, M. Hagler, D. Jurk, L. A. Smith, G. Casacang-Verzosa, Y. Zhu, M. J. Schafer, T. Tchkonja, J. L. Kirkland and J. D. Miller (2016). "Chronic senolytic treatment alleviates established vasomotor dysfunction in aged or atherosclerotic mice." Aging Cell **15**(5): 973-977.
- Roszer, T. (2015). "Understanding the Mysterious M2 Macrophage through Activation Markers and Effector Mechanisms." Mediators Inflamm **2015**: 816460.
- Rtveladze, K. T., S. Marsh, L. M. Barquera, R. Sanchez, D. Levy, G. Melendez, L. Webber, K. F. Kilpi, McPherson and M. Brown (2014). "Obesity prevalence in Mexico: Impact on health and economic burden." Public Health Nutrition **17**: 233-239.
- Rutkowski, M. R., N. Svoronos, A. Perales-Puchalt and J. R. Conejo-Garcia (2015). "The Tumor Microenvironment: Cancer-Promoting Networks Beyond Tumor Beds." Adv Cancer Res **128**: 235-262.
- Salminen, A., K. Kaarniranta and A. Kauppinen (2012). "Inflammaging: disturbed interplay between autophagy and inflammasomes." Aging (Albany NY) **4**(3): 166-175.
- Schafer, M. J., T. A. White, G. Evans, J. M. Tonne, G. C. Verzosa, M. B. Stout, D. L. Mazula, A. K. Palmer, D. J. Baker, M. D. Jensen, M. S. Torbenson, J. D. Miller, Y. Ikeda, T. Tchkonja, J. M. van Deursen, J. L. Kirkland and N. K. LeBrasseur (2016). "Exercise Prevents Diet-Induced Cellular Senescence in Adipose Tissue." Diabetes **65**(6): 1606-1615.
- Schafer, M. J., T. A. White, K. Iijima, A. J. Haak, G. Ligresti, E. J. Atkinson, A. L. Oberg, J. Birch, H. Salmonowicz, Y. Zhu, D. L. Mazula, R. W. Brooks, H. Fuhrmann-Stroissnigg, T. Pirtskhalava, Y. S. Prakash, T. Tchkonja, P. D. Robbins, M. C. Aubry, J. F. Passos, J. L. Kirkland, D. J. Schumperlin, H. Kita and N. K. LeBrasseur (2017). "Cellular senescence mediates fibrotic pulmonary disease." Nat Commun **8**: 14532.



- Sharpless, N. E. and C. J. Sherr (2015). "Forging a signature of in vivo senescence." Nat Rev Cancer **15**(7): 397-408.
- Shaw, A. C., S. Joshi, H. Greenwood, A. Panda and J. M. Lord (2010). "Aging of the innate immune system." Curr Opin Immunol **22**(4): 507-513.
- Shoelson, S. E., J. Lee and A. B. Goldfine (2006). "Inflammation and insulin resistance." J Clin Invest **116**(7): 1793-1801.
- Shulman, G. I. (2000). "Cellular mechanisms of insulin resistance." J Clin Invest **106**(2): 171-176.
- Shuster, A., M. Patlas, J. H. Pinthus and M. Mourtzakis (2012). "The clinical importance of visceral adiposity: a critical review of methods for visceral adipose tissue analysis." Br J Radiol **85**(1009): 1-10.
- Sica, A. and A. Mantovani (2012). "Macrophage plasticity and polarization: in vivo veritas." J Clin Invest **122**(3): 787-795.
- Sica, A., L. Rubino, A. Mancino, P. Larghi, C. Porta, M. Rimoldi, G. Solinas, M. Locati, P. Allavena and A. Mantovani (2007). "Targeting tumour-associated macrophages." Expert Opin Ther Targets **11**(9): 1219-1229.
- Snijder, M. B., P. Z. Zimmet, M. Visser, J. M. Dekker, J. C. Seidell and J. E. Shaw (2004). "Independent and opposite associations of waist and hip circumferences with diabetes, hypertension and dyslipidemia: the AusDiab Study." Int J Obes Relat Metab Disord **28**(3): 402-409.
- Spazzafumo, L., E. Mensa, G. Matakchione, T. Galeazzi, L. Zampini, R. Recchioni, F. Marcheselli, F. Prattichizzo, R. Testa, R. Antonicelli, P. Garagnani, M. Boemi, M. Bonafe, A. R. Bonfigli, A. D. Procopio and F. Olivieri (2017). "Age-related modulation of plasmatic beta-Galactosidase activity in healthy subjects and in patients affected by T2DM." Oncotarget **8**(55): 93338-93348.
- Studencka, M. and J. Schaber (2017). "Senoptosis: non-lethal DNA cleavage as a route to deep senescence." Oncotarget **8**(19): 30656-30671.
- Stumvoll, M., B. J. Goldstein and T. W. van Haeften (2005). "Type 2 diabetes: principles of pathogenesis and therapy." Lancet **365**(9467): 1333-1346.
- Sun, A. R., T. Friis, S. Sekar, R. Crawford, Y. Xiao and I. Prasad (2016). "Is Synovial Macrophage Activation the Inflammatory Link Between Obesity and Osteoarthritis?" Curr Rheumatol Rep **18**(9): 57.
- Sun, J. C., S. Lopez-Verges, C. C. Kim, J. L. DeRisi and L. L. Lanier (2011). "NK cells and immune "memory"." J Immunol **186**(4): 1891-1897.
- Tchkonia, T., N. Giorgadze, T. Pirtskhalava, T. Thomou, M. DePonte, A. Koo, R. A. Forse, D. Chinnappan, C. Martin-Ruiz, T. von Zglinicki and J. L. Kirkland (2006). "Fat depot-specific characteristics are retained in strains derived from single human preadipocytes." Diabetes **55**(9): 2571-2578.
- Tchkonia, T., D. E. Morbeck, T. Von Zglinicki, J. Van Deursen, J. Lustgarten, H. Scrable, S. Khosla, M. D. Jensen and J. L. Kirkland (2010). "Fat tissue, aging, and cellular senescence." Aging Cell **9**(5): 667-684.
- Tchkonia, T., Y. Zhu, J. van Deursen, J. Campisi and J. L. Kirkland (2013). "Cellular senescence and the senescent secretory phenotype: therapeutic opportunities." J Clin Invest **123**(3): 966-972.
- Trayhurn, P. and I. S. Wood (2004). "Adipokines: inflammation and the pleiotropic role of white adipose tissue." Br J Nutr **92**(3): 347-355.

- Vandanmagsar, B., Y. H. Youm, A. Ravussin, J. E. Galgani, K. Stadler, R. L. Mynatt, E. Ravussin, J. M. Stephens and V. D. Dixit (2011). "The NLRP3 inflammasome instigates obesity-induced inflammation and insulin resistance." Nat Med **17**(2): 179-188.
- Villaret, A., J. Galitzky, P. Decaunes, D. Esteve, M. A. Marques, C. Sengenès, P. Chiotasso, T. Tchkonina, M. Lafontan, J. L. Kirkland and A. Bouloumie (2010). "Adipose tissue endothelial cells from obese human subjects: differences among depots in angiogenic, metabolic, and inflammatory gene expression and cellular senescence." Diabetes **59**(11): 2755-2763.
- Wang, K., S. Zhang, J. Weber, D. Baxter and D. J. Galas (2010). "Export of microRNAs and microRNA-protective protein by mammalian cells." Nucleic Acids Res **38**(20): 7248-7259.
- Weisberg, S. P., D. McCann, M. Desai, M. Rosenbaum, R. L. Leibel and A. W. Ferrante, Jr. (2003). "Obesity is associated with macrophage accumulation in adipose tissue." J Clin Invest **112**(12): 1796-1808.
- Wellen, K. E. and G. S. Hotamisligil (2003). "Obesity-induced inflammatory changes in adipose tissue." J Clin Invest **112**(12): 1785-1788.
- Wynn, T. A. and K. M. Vannella (2016). "Macrophages in Tissue Repair, Regeneration, and Fibrosis." Immunity **44**(3): 450-462.
- Yang, Q., T. E. Graham, N. Mody, F. Preitner, O. D. Peroni, J. M. Zabolotny, K. Kotani, L. Quadro and B. B. Kahn (2005). "Serum retinol binding protein 4 contributes to insulin resistance in obesity and type 2 diabetes." Nature **436**(7049): 356-362.
- Yosef, R. and V. Krizhanovsky (2016). "mTOR signaling orchestrates the expression of cytoprotective factors during cellular senescence." Oncotarget **7**(31): 48859.
- Zhang, P., Q. Wang, L. Nie, R. Zhu, X. Zhou, P. Zhao, N. Ji, X. Liang, Y. Ding, Q. Yuan and Q. Wang (2019). "Hyperglycemia-induced inflamm-aging accelerates gingival senescence via NLRC4 phosphorylation." J Biol Chem.
- Zhu, Y., T. Tchkonina, H. Fuhrmann-Stroissnigg, H. M. Dai, Y. Y. Ling, M. B. Stout, T. Pirtskhalava, N. Giorgadze, K. O. Johnson, C. B. Giles, J. D. Wren, L. J. Niedernhofer, P. D. Robbins and J. L. Kirkland (2016). "Identification of a novel senolytic agent, navitoclax, targeting the Bcl-2 family of anti-apoptotic factors." Aging Cell **15**(3): 428-435.
- Zhu, Y., T. Tchkonina, T. Pirtskhalava, A. C. Gower, H. Ding, N. Giorgadze, A. K. Palmer, Y. Ikeno, G. B. Hubbard, M. Lenburg, S. P. O'Hara, N. F. LaRusso, J. D. Miller, C. M. Roos, G. C. Verzosa, N. K. LeBrasseur, J. D. Wren, J. N. Farr, S. Khosla, M. B. Stout, S. J. McGowan, H. Fuhrmann-Stroissnigg, A. U. Gurkar, J. Zhao, D. Colangelo, A. Dorransoro, Y. Y. Ling, A. S. Barghouthy, D. C. Navarro, T. Sano, P. D. Robbins, L. J. Niedernhofer and J. L. Kirkland (2015). "The Achilles' heel of senescent cells: from transcriptome to senolytic drugs." Aging Cell **14**(4): 644-658.
- Ziegler-Heitbrock, L., P. Ancuta, S. Crowe, M. Dalod, V. Grau, D. N. Hart, P. J. Leenen, Y. J. Liu, G. MacPherson, G. J. Randolph, J. Scherberich, J. Schmitz, K. Shortman, S. Sozzani, H. Strobl, M. Zembala, J. M. Austyn and M. B. Lutz (2010). "Nomenclature of monocytes and dendritic cells in blood." Blood **116**(16): e74-80.